Toxicon 205 (2022) 38–52

Contents lists available at ScienceDirect

Toxicon

journal homepage: www.elsevier.com/locate/toxicon

An integrative view of the toxic potential of *Conophis lineatus* (Dipsadidae: Xenodontinae), a medically relevant rear-fanged snake

Tristan D. Schramer [a,**], Rhett M. Rautsaw [a], Juan David Bayona-Serrano [b], Gunnar S. Nystrom [c], Taylor R. West [d], Javier A. Ortiz-Medina [e,f,g], Bianca Sabido-Alpuche [f], Marcos Meneses-Millán [f], Miguel Borja [h], Inácio L.M. Junqueira-de-Azevedo [b,i], Darin R. Rokyta [c], Christopher L. Parkinson [a,j,*]

[a] *Department of Biological Sciences, Clemson University, Clemson, SC, USA*
[b] *Laboratório de Toxinologia Aplicada, Instituto Butantan, São Paulo, Brazil*
[c] *Department of Biological Science, Florida State University, Tallahassee, FL, USA*
[d] *Department of Ecology and Evolutionary Biology, University of Michigan, Ann Arbor, MI, USA*
[e] *Departamento de Sistemática y Ecología Acuática, El Colegio de La Frontera Sur, Unidad Chetumal, Chetumal, Quintana Roo, Mexico*
[f] *Unidad de Manejo para La Conservación de La Vida Silvestre, Tsáab Kaan, Baca, Yucatán, Mexico*
[g] *HERP.MX A.C., Villa de Álvarez, Colima, Mexico*
[h] *Facultad de Ciencias Biológicas, Universidad Juárez Del Estado de Durango, Gómez Palacio, Durango, Mexico*
[i] *Center of Toxins, Immune-Response and Cell Signaling (CeTICS), São Paulo, Brazil*
[j] *Department of Forestry and Environmental Conservation, Clemson University, Clemson, SC, USA*

ARTICLE INFO

Handling Editor: Ray Norton

Keywords:
Road guarder
Duvernoy's venom gland
RNA-Seq
Venomics
Venom characterization
Envenomation

ABSTRACT

Most traditional research on snake venoms has focused on front-fanged snake families (Viperidae, Elapidae, and Atractaspididae). However, venom is now generally accepted as being a much more broadly possessed trait within snakes, including species traditionally considered harmless. Unfortunately, due to historical inertia and methodological challenges, the toxin repertoires of non-front-fanged snake families (e.g., Colubridae, Dipsadidae, and Natricidae) have been heavily neglected despite the knowledge of numerous species capable of inflicting medically relevant envenomations. Integrating proteomic data for validation, we perform a *de novo* assembly and analysis of the Duvernoy's venom gland transcriptome of the Central American Road Guarder (Dipsadidae: Xenodontinae: *Conophis lineatus*), a species known for its potent bite. We identified 28 putative toxin transcripts from 13 toxin families in the Duvernoy's venom gland transcriptome, comprising 63.7% of total transcriptome expression. In addition to ubiquitous snake toxin families, we proteomically confirmed several atypical venom components. The most highly expressed toxins (55.6% of total toxin expression) were recently described snake venom matrix metalloproteases (svMMPs), with 48.0% of svMMP expression contributable to a novel svMMP isoform. We investigate the evolution of the new svMMP isoform in the context of rear-fanged snakes using phylogenetics. Finally, we examine the morphology of the venom apparatus using μCT and explore how the venom relates to autecology and the highly hemorrhagic effects seen in human envenomations. Importantly, we provide the most complete venom characterization of this medically relevant snake species to date, producing insights into the effects and evolution of its venom, and point to future research directions to better understand the venoms of 'harmless' non-front-fanged snakes.

1. Introduction

Front-fanged snake families (Viperidae, Elapidae, and Atractaspididae) with genera such as *Bothrops* (lanceheads), *Crotalus* (rattlesnakes), *Echis* (saw-scaled vipers), *Naja* (cobras), and *Micrurus* (coral snakes) have been the focus of most snake venom research due to their medical significance. However, the venom system likely arose in an ancestral snake, or perhaps an early toxicoferan (Fry et al., 2006; Jackson et al.,

* Corresponding author. Department of Biological Sciences, Clemson University, Clemson, SC, USA.
** Corresponding author.
E-mail addresses: tdschra@clemson.edu (T.D. Schramer), viper@clemson.edu (C.L. Parkinson).

https://doi.org/10.1016/j.toxicon.2021.11.009
Received 9 August 2021; Received in revised form 25 October 2021; Accepted 10 November 2021
Available online 15 November 2021

2017; Vidal, 2002; Vonk et al., 2008). Therefore, these front-fanged snakes represent a trivial proportion of the total venomous reptile diversity which biases our understanding of venom evolution, including the origins, diversification, and novelty of venom gene families (Jackson et al., 2019). From this frame of reference, the toxin repertoire of non-front-fanged snake (NFFS) families (e.g., Colubridae, Dipsadidae, and Natricidae) has been heavily neglected (Junqueira-de-Azevedo et al., 2016). Non-front-fanged snakes are generally more challenging to study because the Duvernoy's venom gland (DVG), unlike the venom gland of vipers and elapids, generally lacks the anatomy for the storage and rapid delivery of large quantities of venom (Modahl and Mackessy, 2019; Weinstein et al., 2010), although both are homologous tissues (Jackson et al., 2017). Instead, venom is passively secreted from the oral gland to enlarged, posterior maxillary teeth (Modahl and Mackessy, 2019). Nonetheless, many NFFSs are considered medically relevant and in need of additional research on their venom composition (Minton, 1990; Modahl and Mackessy, 2019; Weinstein et al., 2011).

In the Old World, several species of NFFSs are considered highly venomous and potentially lethal to humans including boomslangs (Colubridae: *Dispholidus typus*), twig snakes (Colubridae: *Thelotornis*), and keelbacks (Natricidae: *Rhabdophis*) (Jackson et al., 2019; Modahl and Mackessy, 2019; Weinstein et al., 2011). Other Old World species such as cat snakes (Colubridae: *Boiga*) are also highly venomous; however, the venom of these arboreal snakes is generally specialized for eating birds and lizards, rather than mammalian prey (Dashevsky et al., 2018; Mackessy et al., 2006; McGivern et al., 2014). In the New World, very few NFFS species are considered medically significant; however, envenomations by some taxa (e.g., *Philodryas, Heterodon*, *Helicops*, *Hydrops*) have caused local and potentially systemic effects that require medical attention (da Graça Salomão et al., 2003; de Medeiros et al., 2021; Gutiérrez and Sasa, 2002; Prado-Franceschi and Hyslop, 2002; Villca-Corani et al., 2021; Warrell, 2004; Weinstein et al., 2011). Moreover, taxon-specific toxins specialized for different prey resources, ontogenetic shifts in venom composition, and geographic variation are now known to occur in NFFS venoms (e.g., Heyborne and Mackessy, 2021; Hofmann et al., 2021; Mackessy et al., 2006; Modahl et al., 2018b). Unfortunately, NFFSs remain underappreciated in toxinological studies despite representing the majority of extant snake diversity—with over 2400 species (Uetz, 2010; Uetz et al., 2020; Uetz and Stylianou, 2018; Zaher et al., 2019).

At the time their review was published, Modahl et al. (2020) reported 65 published venom gland transcriptomes for snakes of which 50 (77%) were from front-fanged snake families and 15 (23%) were from NFFS families. Breakthroughs in proteomic and genomic technologies has facilitated our ability to examine the venom repertoire with only small amounts of venom or venom gland tissue (Hofmann et al., 2021; Modahl et al., 2018a, 2020; Modahl and Mackessy, 2019). This has led to the discovery of entirely new venom components as well as toxin families in the venom of NFFSs, such as lactadherins (Lacta) and snake venom matrix metalloproteases (svMMPs) (Ching et al., 2012; Junqueira-de-Azevedo et al., 2016; Komori et al., 2006; Mackessy, 2002). In particular, these new venom constituents were discovered in several genera of Dipsadidae (Xenodontinae)—*Erythrolamprus*, *Gomesophis*, *Lygophis*, *Ptychophis*, *Thamnodynastes*, *Tomodon*, and *Xenodon* (Bayona-Serrano et al., 2020; Bayona-Serrano et al., 2019; Junqueira-de-Azevedo et al., 2016).

The tribe Conophiini is a clade of xenodontine snakes (Dipsadidae: Xenodontinae), sister to all other xenodontine snakes (Zaher et al., 2019). Conophiini includes the genus *Conophis* and, pending more comprehensive molecular studies, possibly *Crisantophis* and *Manolepis* (Grazziotin et al., 2012; Zaher et al., 2019). *Conophis*, in particular, contains three diurnal, rear-fanged snake species—*C. lineatus*, *C. vittatus*, and *C. morai*—which are endemic to Middle America (but see Wilson and Johnson, 2012 and Heimes, 2016 regarding the taxonomic status of

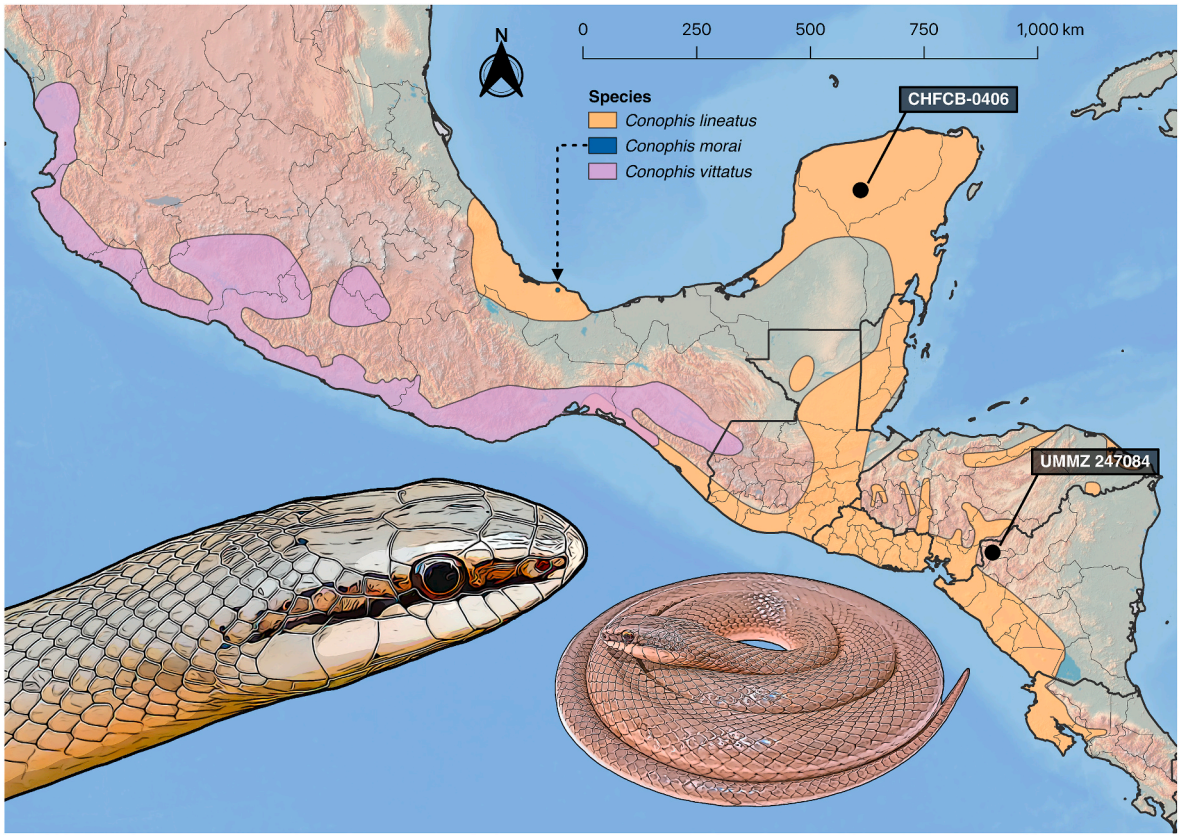

Fig. 1. Distribution of the genus *Conophis*. Specimens used in venomic (CHFCB-0406) and morphological (UMMZ 247084) investigations are indicated with black points and labeled accordingly. Inset images by Tristan D. Schramer, based on photographs by Aníbal H. Díaz de la Vega P. and Rhett M. Rautsaw, respectively.

C. morai) (Fig. 1).

The Central American Road Guarder (*C. lineatus*), or Guarda Caminos Centroamericana, ranges from Mexico to Costa Rica (Fig. 1), reaching a maximum total length of 1167 mm (Wellman, 1963). *Conophis lineatus* feeds primarily on lizards; however, it is known as a generalist feeder which never refuses a meal (Mittleman, 1944; Pérez-Alvarado and Vásquez-Cruz, 2021; Stafford and Henderson, 2006). Importantly, this species produces a venom which has manifested in mild to severe local effects in humans (Cook, 1984; Gutiérrez and Sasa, 2002; Johanbocke, 1974; Johnson, 1988; Taylor and Smith, 1938). Specifically, most bites from *C. lineatus* result in an immediate burning pain at the site of the bite, bleeding, and edema (Warrell, 2004; Weinstein et al., 2011). Pain and swelling often last for hours to days accompanied by persistent bleeding, suggesting a possible anticoagulant effect (Gutiérrez and Sasa, 2002; Johanbocke, 1974). Despite the clear medically relevant venom present in *Conophis*, no study has ever characterized the venom of this species.

Herein, we use DVG transcriptomics and venom proteomics to characterize the venom of *C. lineatus* with a single individual captured near Sotuta, Yucatán, Mexico (Fig. 1). We uncover the presence of snake venom matrix metalloproteases (svMMPs) and describe a new isoform resulting from a partial domain deletion. Moreover, we identify the occurrence of several atypical venom components (putative toxins) along with the known typical, ubiquitous snake toxins and discuss their potential roles in the venom. We also examine the morphology of the DVG and rear-fangs from a specimen collected in Nicaragua (Fig. 1), assess aspects of the venom delivery system of *C. lineatus*, and consider their implications. Finally, we explore the venom composition and delivery system of *C. lineatus* in the context of its autecology and cases of human envenomation to try and connect behavior, biological activity, and potential function to these observations.

2. Materials and methods

2.1. Sample collection

During June of 2018, we collected a single adult *Conophis lineatus* (snout-vent length [SVL] = 700 mm; total length = 875 mm; mass = 124 g) near Sotuta, Yucatán, México and processed it in preparation for DVG transcriptome sequencing. We collected venom by modifying the protocols of Rosenberg (1992) and Hill and Mackessy (1997). First, we anesthetized the animal with isoflurane and administered a subcutaneous injection of pilocarpine (6 μg/g of the snake's mass), a parasympathetic stimulator, in the anterior portion of the body. Saliva was then collected from the mouth using a micropipette and two polished capillary tubes were placed onto the rear fangs for venom collection. Once the venom was obtained, it was vacuum dried and stored at −80 °C for future use. Four days after venom was collected and transcription was maximized (Rotenberg et al., 1971), we euthanized the animal using an intracoelomic injection of 1% tricaine mesylate (MS-222) followed by another 50% injection after anesthesia (Conroy et al., 2009). We subsequently removed the DVGs and stored them separately in RNAlater (Thermo Fisher Scientific, Waltham, MA, USA) at 4 °C overnight before moving to −80 °C for long-term storage. The specimen was fixed in 10% buffered formalin for five days and then transferred to 70% ethanol and deposited in the Colección Herpetológica, Facultad de Ciencias Biológicas, Universidad Juárez del Estado de Durango (CHFCB-0406).

2.2. Duvernoy's venom gland transcriptome sequencing

Total RNA was extracted from left and right DVGs independently using a standard TRIzol extraction following Hofmann et al. (2018). In brief, DVGs were finely diced and placed in TRIzol solution (Invitrogen, Carlsbad, CA, USA). We then homogenized the mixture and transferred it to a phase lock heavy gel tube (5 PRIME; No 2302830, Quantabio, Beverly, MA, USA). Once the cells were lysed, total RNA was separated using chloroform and purified via isopropyl alcohol and ethanol precipitation. To ensure sufficient quantity and quality RNA for library preparation and sequencing, we estimated the concentration of total RNA using a Qubit RNA BroadRange Assay (Thermo Fisher Scientific) and evaluated RNA quality and concentration using an Agilent Bioanalyzer 2100 with the RNA 6000 Pico Kit (Agilent Technologies, Santa Clara, CA, USA).

We produced cDNA libraries from isolated mRNA using magnetic bead isolation of mRNA followed by cDNA synthesis and PCR amplification (see Rokyta et al., 2017, 2015, 2012). First, we isolated mRNA using the NEBNext Poly(A) mRNA Magnetic Isolation Module (NEB #E7490S; New England Biolabs, Ipswich, MA, USA) with equal amounts of mRNA from the left and right DVGs. Following bead isolation and cleanup, cDNA libraries were prepared from isolated mRNA using a NEBNext Ultra RNA Library Prep Kit for Illumina (NEB #E7530) following the manufacturer's protocols. We used a fragmentation time of 13.5 min to achieve a target mean fragment size of 400 bp and 14 PCR cycles for amplification of double stranded cDNA libraries. The library yield and quality were quantified on a Bioanalyzer 2100 with the DNA High Sensitivity Kit (Agilent Technologies). The total amplifiable concentration of cDNA in each library was then determined using KAPA qPCR (Roche KK4873) at the Florida State University Molecular Cloning Facility. Samples were pooled for sequencing and the final concentration and quality of the pooled library samples were then assessed on the Bioanalyzer and via KAPA qPCR. Pooled libraries were sequenced with 150 base pair (bp) paired-end reads on an Illumina NovaSeq 6000 platform at the Florida State University College of Medicine Translational Science Laboratory (Tallahassee, FL, USA).

2.3. Transcriptome assembly and annotation

A combination of custom python scripts and established software were used to clean and assemble the raw reads and assess the resulting contigs. The raw 150 bp paired-end reads were first trimmed to keep reads with a length greater than 75 bp and base calls with a phred score of 5 or greater using Trim Galore! v. 0.4.4 (https://github.com/FelixKrueger/TrimGalore). Next, paired-end reads were merged using PEAR v. 0.9.10 (Zhang et al., 2014). The trimmed, merged reads were *de novo* assembled using three different methods to maximize toxin assembly following Holding et al. (2018): Extender (Rokyta et al., 2012), DNAStar SeqMan NGen v. 14 using default settings (Lasergene DNAStar software package; DNASTAR Inc, Madison, WI, USA), and Trinity v. 2.9 (Grabherr et al., 2011; Haas et al., 2013). Extender assemblies used 1000 merged reads as seeds, extending the seeds based on exact overlaps of 120 base pairs.

Assemblies were then combined and contigs were sorted into toxins and non-toxins via blastx searches against the UniProt animal venom proteins and toxins database (http://www.uniprot.org/program/Toxins) with a minimum e-value of 10^{-4}. Both toxins and non-toxins (e.g., housekeeping genes) were then annotated by clustering sequences using cd-hit-est (Fu et al., 2012) to a database of previously annotated snake toxin and *Crotalus horridus* non-toxin transcripts (Rokyta et al., 2013). Sequences and associated signal peptides with a match percentage of 80 were automatically annotated. The remaining toxin contigs were manually annotated in Geneious v. 2019.2.3 (Biomatters Ltd, Auckland, New Zealand) by comparing the sequences to the blastx results. Any atypical venom components were checked for signal peptides using SignalP v. 4.1 (Petersen et al., 2011) with default settings.

We then combined annotated toxins and non-toxins, removed duplicate sequences, and screened for chimeric sequences by aligning merged reads to the annotated transcripts using BWA-MEM (Li, 2013), removing reads with any mismatches via gaps or nucleotide differences. Transcripts with zero coverage at any base were automatically flagged and removed. Chimeric transcripts were reported by searching for a difference of greater than 75% in the average length of reads on either

side of a given site across a transcript based on the average read size (https://github.com/masonaj157/ChimeraKiller). The remaining transcripts were clustered with a sequence identity threshold of 99% using cd-hit to reduce redundancy of repeat transcripts and cluster allelic variation at single loci to produce our final transcriptome (Fu et al., 2012).

Finally, to check for potentially missing high-expression transcripts in our final transcriptome, we identified all open-reading frames (ORFs) in our combined assembly with emboss getorf (Rice et al., 2000). We then estimated expression of all ORFs with RSEM and compared the top 100 most highly expressed ORFs with our final transcriptome. Novel, non-chimeric ORFs were then added to our final transcriptome.

2.4. Expression analysis and visualization

Relative expression of toxin and non-toxin genes was calculated by mapping merged reads to the final transcript set with Bowtie 2 (Langmead and Salzberg, 2012) in RSEM v. 1.3.0 (Li and Dewey, 2011). We used the transcripts per million reads (TPM) data as our abundance estimates. We imported the dataset into RStudio v. 1.2.5033 using R v. 4.0.0 (R Core Team, 2013). We removed two non-toxin transcripts with zero TPM. We then performed a log transformation of the TPM data and plotted expression of each transcript and calculated the proportional expression of each toxin family. Dataset manipulation was done using the R package 'dplyr' (Wickham et al., 2020) and plotting done using 'ggpubr' (Kassambara, 2019) and 'patchwork' (Pedersen, 2020).

2.5. Venom proteomics

Reversed-phase high-performance liquid chromatography (RP-HPLC) was performed on the single venom sample from *C. lineatus* using the Prominence HPLC System (Shimadzu Scientific Instruments, Kyoto, Kyoto, Japan). We resuspended the dry venom in water and removed insoluble material via centrifugation. We determined the concentration of the venom using a Nanodrop 2000c Spectrophotometer (ThermoFisher Scientific). Then, approximately 15 μg of protein was injected onto an Aeris 3.6 μm WIDEPORE XB-C18 (250 mm length; 2.1 mm internal diameter) column (Phenomenex, Torrance, CA) utilizing the SIL-30 AC autosampler, a standard solvent system of A = 0.1% trifluoroacetic acid (TFA) in water and B = 0.06% TFA in acetonitrile, and a detection wavelength of 220 nm. All samples were run using a flow rate of 0.2 mL/min over a 125-min gradient starting at 10% B for 5 min. The gradient was then increased from 10% B to 55% over 110 min and increased again to 75% B over 5 min. Finally, the gradient was kept at 75% B for an additional 5 min before performing a 15-min wash step using 10% B.

To confirm toxin presence in the venom proteome and produce a genotype-to-phenotype map, we implemented quantitative mass spectrometry (qMS) on our whole *C. lineatus* venom sample following Margres et al. (2021). We used a Nanodrop 2000c Spectrophotometer (ThermoFisher Scientific) to quantify venom protein concentrations. First, we added 11 μg of venom to 150 μL of 100 mM Ammonium Bicarbonate for 20 min. Next, we added 30 μL of 10 mM DTT (Dithiothreitol) and incubated for 1 h at 60 °C. After incubation, we added 30 μL of 50 mM IAA (Iodoacetoamine), followed by 150 μL of 50 mM Ammonium Bicarbonate 30 min later. Trypsin (Promega V511 at 0.5 μg/2.5 μL) diluted in 50 mM Ammonium Bicarbonate was then added to begin digestion and incubated for 18 h at 37 °C. Finally, we added 1% TFA (Trifluoroacetic acid) at 5% volume of the solution to stop digestion. The sample was subsequently dried using a SpeedVac at 25 °C for 1 h and stored at −20 °C until use. The resulting dried and digested tryptic peptides were redissolved in 0.1% formic acid at a final concentration of 250 ng/μL in preparation for mass spectrometry. Three digested *Escherichia coli* proteins, which were purchased from Abcam (Waltham, MA) at known concentrations and mixed in the specified proportions (1000×) prior to digestion, were used as internal standards: 25 fmol of P00811 (Beta-lactamase ampC), 250 fmol of P31658 (Protein deglycase 1), and 2500 fmol of P31697 (Chaperone protein FimC) per injection. The internal standard peptide mix was then infused into the sample to yield the selected final concentration.

For the LCMS/MS run, a 2 μL aliquot was analyzed using an externally calibrated Thermo Q Exactive HF (high-resolution electrospray tandem mass spectrometer) in conjunction with the Dionex UltiMate 3000 RSLCnano System. The 2 μL sample was aspirated into a 50 μL loop and loaded onto the trap column (Thermo μ-Precolumn 5 mm, with nanoViper tubing 30 μm i. d. × 10 cm). For separation on the analytical column (Acclaim pepmap RSLC 75 μMx 15 cm nanoviper), the flow rate was set to 300 nl/min. Mobile phase A was composed of 99.9% H2O (EMD Omni Solvent) and 0.1% formic acid, and mobile phase B was composed of 99.9% ACN and 0.1% formic acid. We performed a 60 min linear gradient from 3% to 45% B. The LC eluent was directly nanosprayed into the Q Exactive HF mass spectrometer (Thermo Scientific). During the chromatographic separation, the Q Exactive HF was operated in a data-dependent mode and under direct control of the Thermo Excalibur 3.1.66 (Thermo Scientific). Resulting MS data were acquired using a data-dependent top-20 method for the Q Exactive HF platform, dynamically choosing the most abundant not-yet-sequenced precursor ions from the survey scans. Sequencing was performed via higher energy collisional dissociation fragmentation with a target value of 10^5 ions determined with predictive automatic gain control. Full scans (350–1700 m/z) were performed at 60,000 resolution in profile mode. MS2 were acquired in centroid mode at 15,000 resolution. We excluded ions with a single charge, charges greater than seven, or an unassigned charge. A 15-s dynamic exclusion window was used. All measurements were performed at room temperature with three technical replicates to facilitate label-free quantification and account for machine-related variability.

We searched the resulting raw files with Proteome Discoverer v. 2.2 (ThermoFisher Scientific) using SequestHT as the search engine with custom-generated FASTA databases and percolator as the peptide validator. Searches were performed twice, first with all open-reading frames (ORFs) in the transcriptome assembly identified by emboss (getorf -find 1 -minsize 90; Rice et al., 2000) to check for potential missing toxins in our transcriptome. The second search was done against our final transcriptome, including the curated toxin sequences, to proteomically confirm the presence of each toxin in the venom. We used the following SequestHT search parameters: enzyme name = Trypsin, maximum missed cleavage = 2, minimum peptide length = 6, maximum peptide length = 144, maximum delta Cn = 0.05, precursor mass tolerance = 10 ppm, fragment mass tolerance = 0.2 Da, dynamic modifications, carbamidomethyl +57.021 Da(C), and oxidation + 15.995 Da(M). Protein identities were validated using Scaffold v. 4.10.0 (Proteome Software Inc, Portland, OR, USA). We accepted protein identities based on a 1.0% false discovery rate (FDR) using the Scaffold Local FDR algorithm and a minimum of one recognized peptide. We considered a transcript proteomically detected if it was found in at least one of the three replicates. Proteins grouped by Scaffold due to shared peptide evidence were treated individually rather than as a cluster to allow us to directly assign the peptide to the corresponding transcript.

2.6. svMMP confirmation & phylogenetics

To validate that the presence of any new svMMP isoforms were not the result of mis-assembly, we again checked for chimeras as above. Specifically, we searched for a difference of greater than 75% in the average length of reads on either side of a given site across a transcript based on the average read size (https://github.com/masonaj157/ChimeraKiller). We then manually searched for reads spanning the unique portions at the end and beginning of the domains bridging the putative gap. If no reads spanned this region, it would suggest mis-assembly and that isoform may be chimeric. To further confirm the presence of new isoforms in the venom, we similarly used the qMS peptide sequences to

search for peptides that span the end and beginning of the domains bridging the alledged gap.

To examine the evolution of *C. lineatus* svMMPs, we joined our recovered transcripts with the curated snake matrix metalloprotease (snake endogenous MMP-9-like and svMMP) dataset investigated by Bayona-Serrano et al. (2020). MMP sequences were aligned using MAFFT v. 7.450 (Katoh et al., 2002; Katoh and Standley, 2013) in Geneious v. 2020.2.2 (Biomatters Ltd, Auckland, New Zealand) with default parameters. Phylogenetic tree reconstruction was done using IQ-TREE v. 2.0.3 (Minh et al., 2020; Nguyen et al., 2015) with ModelFinder (Kalyaanamoorthy et al., 2017) and 100 non-parametric bootstrap replicates (Fig. S1; Document S1).

2.7. Venom delivery system computed tomography

We collected morphological data regarding the venom delivery system of *C. lineatus* using diffusible iodine-based contrast enhanced and micro-computed tomography (diceCT and μCT). We selected an adult (SVL = 631 mm), preserved museum specimen housed at the University of Michigan Museum of Zoology—UMMZ 247084, collected from Brisas del Mogotón, Nueva Segovia, Nicaragua. The specimen was stained in 1.25% Lugol's iodine solution for 7 days in order to saturate soft tissues for inspection (Callahan et al., 2021). The specimen was then scanned using a high-resolution industrial CT scanner—the University of Michigan operates a Nikon XT H 225 ST μCT Scanner (maximum resolution: 3–5 μm; maximum Kilo-Volts: 225 kV). The *C. lineatus* voxel size was 24.29 μm and 3141 total projections were created. Image stacks and 3-Dimensional renderings were then created using Dragonfly v. 2021.1.0.977 segmentation software (Object Research Systems [ORS] Inc, Montreal, Canada; software available at http://www.theobjects.com/dragonfly). The DVG was segmented from the rest of the specimen using the grayscale thresholding selection tool and highlighted to show location within the organism's head. Corresponding skeletal μCT scan data for this specimen can be found on MorphoSource.org (ark:/87,602/m4/M68551; ummz:herps:247,084).

2.8. Human bite cases

We reviewed *Conophis* bite cases from both the literature and personal communications and interpreted associated sequelae. See Document S2 for specific details and an overview regarding how each source was interpreted.

3. Results and discussion

3.1. Venom RP-HPLC

We obtained approximately 50 μL of translucent secretions from the rear fangs of the *C. lineatus* used in this study. RP-HPLC analysis of the oral secretions revealed multiple peaks and high complexity, particularly of proteins eluting between 75 and 110 min (Fig. 2e). Previous studies have shown that proteins eluting in this time range are relatively large, such as P-III snake venom metalloproteases (SVMPIIIs), with sizes up to 75 kDa (Borja et al., 2018). We expect that the SVMPIIIs present in *C. lineatus* are similarly represented in this range as well as slightly smaller proteins such as SVSPs and svMMPs. However, we could not confirm the identity of each peak.

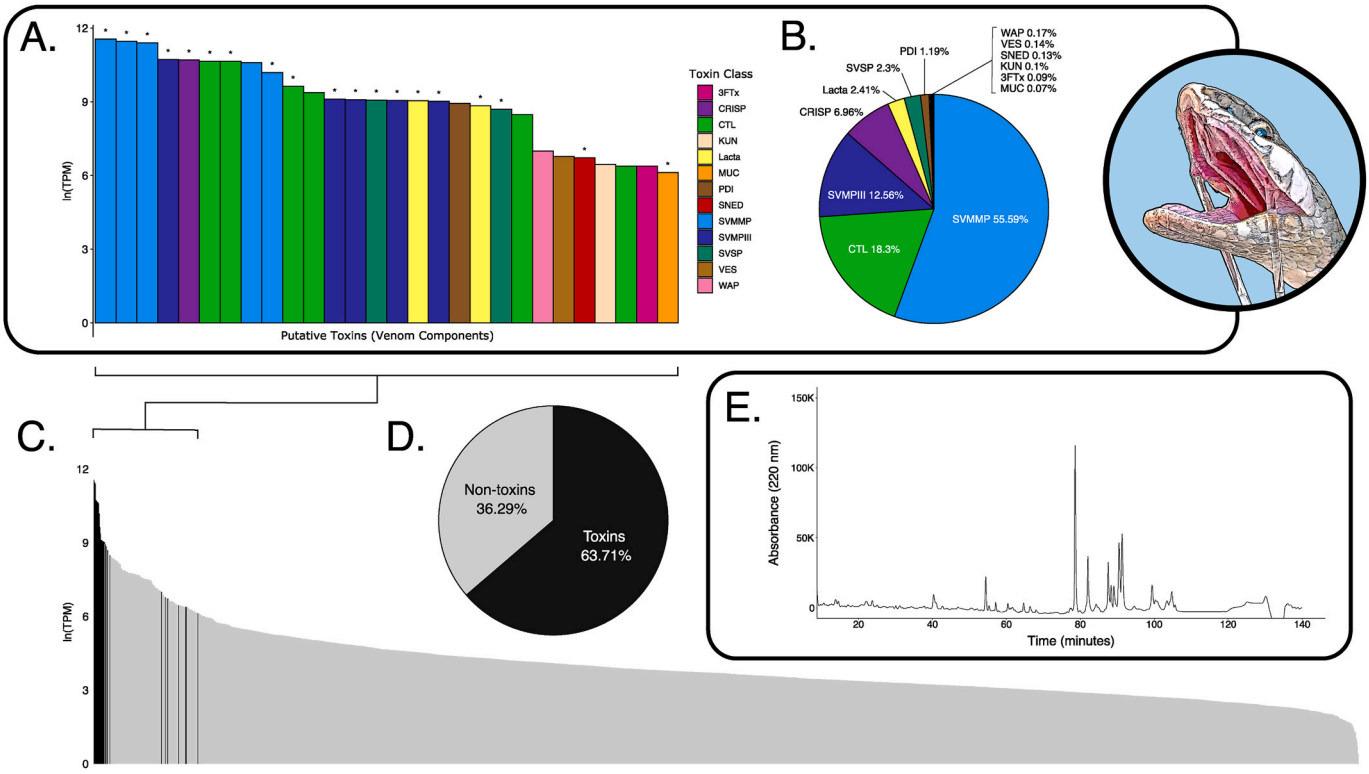

Fig. 2. Venom characterization of *Conophis lineatus*. (A) Ranked expression of the 28 recovered putative toxin (venom component) transcripts present in the Duvernoy's venom gland (DVG) transcriptome of *C. lineatus* colored by toxin class. Asterisks (*) denote proteomically confirmed transcripts. (B) The proportion of each toxin class expressed in the DVG transcriptome. (C) Ranked expression of toxin and non-toxin transcripts in the DVG transcriptome—the majority of the highly expressed transcripts are toxins. (D) The proportion of toxins and non-toxins expressed in the DVG transcriptome. (E) RP-HPLC profile for C. lineatus venom, exhibiting complexity when SVMPs and svMMPs elute. Inset image by Tristan D. Schramer, based on photograph by Rhett M. Rautsaw. Abbreviations: Three-Finger Toxin (3FTx); Cystine Rich Secretory Protein (CRISP); C-Type Lectin (CTL); Kunitz-like protein (KUN); Lactadherin (Lacta); Mucin-like protein (MUC); Protein Disulfide Isomerase (PDI); Sushi, Nidogen and EGF-like Domain-containing protein (SNED); Snake Venom Matrix Metalloprotease (SVMMP); P-III subclass Snake Venom Metalloprotease (SVMPIII); Snake Venom Serine Protease (SVSP); Vespryn (VES); Waprin-like protein (WAP).

3.2. Duvernoy's venom gland transcriptome and venom composition

Combining tissues from both the right and left DVGs, we sequenced the DVG transcriptome. We generated over 17 million raw read pairs using 150 bp paired-end transcriptome sequencing on the Illumina NovaSeq platform, which yielded over 14 million merged reads that passed the quality filter and had overlapping 3′ ends. After assembly, annotation, duplicate and chimera removal, and clustering, our consensus *C. lineatus* transcriptome consisted of 1943 putative non-toxins and 28 putative toxins (19 proteomically confirmed in the venom) from 13 gene families (Fig. 2; Table S1).

Most highly expressed in the transcriptome were snake venom matrix metalloproteases (svMMPs; Fig. 2a), a recently discovered snake venom protein family that constituted 55.6% of toxin expression (Fig. 2b). C-type lectins (CTLs) were the second most highly expressed toxin family at 18.3%, followed by P-III subclass snake venom metalloproteases (SVMPIIIs) at 12.6%, a cystine-rich secretory protein (CRiSP) at 6.7%, lactadherin-like proteins (Lactas) at 2.4%, and snake venom serine proteases (SVSPs) at 2.3% (Fig. 2b). Trace amounts of the following components constituted the remaining 1.9% of the elements expressed in the transcriptome: protein disulfide isomerase (PDI); waprin-like protein (WAP); vespryn (VES); sushi, nidogen and EGF-like domain-containing protein (SNED); kunitz-type protein (KUN); three-finger toxin (3FTx); and a mucin-like protein (MUC).

The most diverse toxin families were as follows: CTLs, with six different putative toxins identified; SVMPIIIs and svMMPs, both with five different putative toxins identified; and SVSPs and Lactas, each with two identified transcripts (Fig. 2a). The 19 proteomically confirmed toxins included four svMMPs, one CRiSP, five SVMPIIIs, three CTLs, two SVSPs, two Lactas, one SNED, and one MUC (Fig. 2a).

3.3. Snake venom matrix metalloproteases

Snake venom matrix metalloproteases constituted five different toxins identified in the transcriptome, with four being proteomically confirmed. A Bayona Serrano et al. (2020) described two sequential forms of svMMPs (svMMP-As and svMMP-Bs) marked by the loss of the hemopexin domain, and subsequently, the fibronectin repeats, respectively (Fig. 3b). Of the svMMPs found in the *C. lineatus* transcriptome, two match the description of svMMP-As in lacking their hemopexin domain (Bayona-Serrano et al., 2020). The remaining three do not adhere to the currently described forms.

Like all described svMMPs to date, the new svMMP isoform—hereafter svMMP type C (svMMP-C)—represents a snake endogenous MMP-9 (seMMP-9) derivative with the loss of the hemopexin domain. However, unlike the svMMP-A, which maintains three fibronectin repeats (F2Ns), the svMMP-C has lost the middle fibronectin repeat, and thus, possesses two rather than three F2Ns (Fig. 3b). To confirm that the presence of the svMMP-C isoform—or the loss of the middle fibronectin repeat (FN2b)—was not the result of mis-assembly, we again checked for chimeras as described in the methods and manually searched for reads spanning the unique portions at the end of FN2a and the beginning of FN2c. We similarly used the qMS peptide sequences to search for peptides that span the end of FN2a and beginning of FN2c.

Both secondary validations supported the correct assembly and non-chimeric nature of svMMP-Cs. Two of the three unique svMMP-C transcripts were proteomically confirmed, with a qMS-derived peptide sequence spanning the gap between the first and third fibronectin repeat, supporting its validity. One of these proteomically confirmed svMMP-Cs also contained a deletion within the catalytic domain, but without a qMS-sequenced peptide flanking the gap, we refrain from formally describing it as another isoform and recognize it as a svMMP-C until further analyses verify its authenticity.

To explore the evolutionary origins of svMMP-Cs and their relationship to other related MMPs, we inferred a maximum likelihood phylogeny of seMMP-9s, svMMP-As, svMMP-Bs, and svMMP-Cs using complete protein DNA coding regions. The results, summarized in the gene tree in Fig. 3a, were consistent with the relationships detailed in a Bayona Serrano et al. (2020) with three apparent origins of svMMPs within the three tribes from which svMMPs are known to be highly

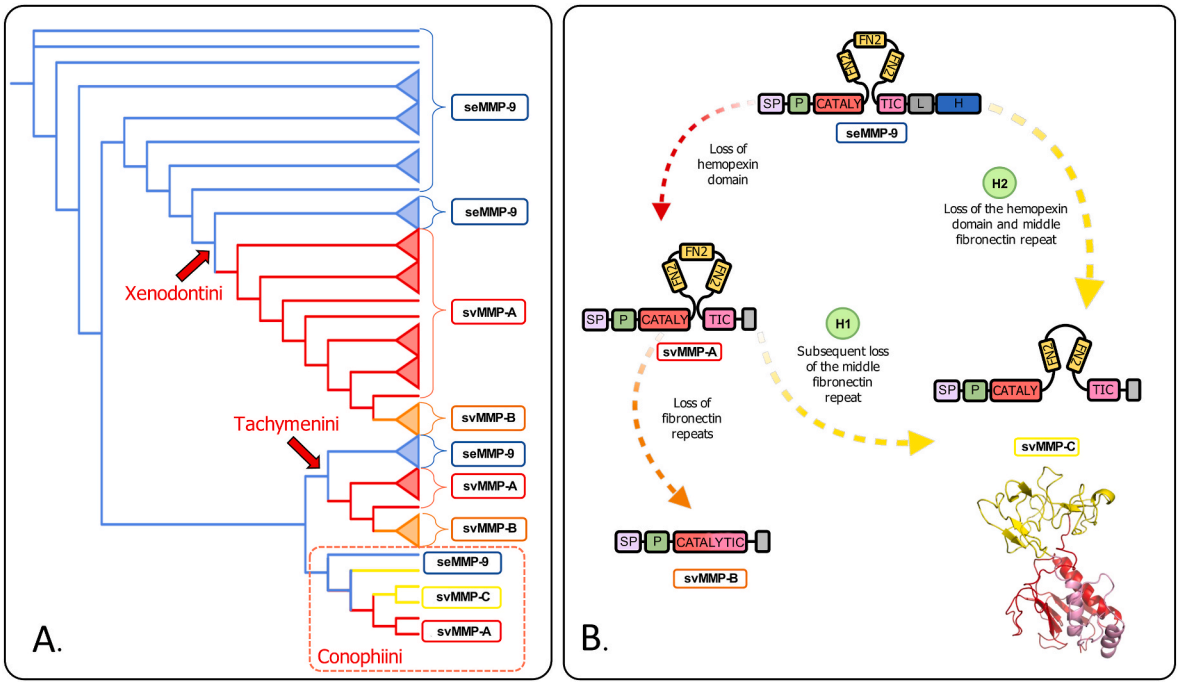

Fig. 3. Evolution of svMMPs. (A) Schematic ML gene tree of snake endogenous MMP-9s and svMMPs showing the phylogenetic relationships between the three types of proteins. (B) Proposed evolution of svMMPs through sequential domain losses (Bayona-Serrano, 2020) considering alternative hypotheses (H1 and H2) for the origin of svMMP-C. The labeled boxes represent the domains that compose the protein. Abbreviations: signal peptide (SP), prodomain (P), catalytic domain I (CATALY), fibronectin (FN2), catalytic domain II (TIC), linker (L), hemopexin (H)\ snake venom matrix metalloprotease (svMMP), type A (svMMP-A), type B (svMMP-B), type C (svMMP-C), snake endogenous matrix metalloprotease 9 like protein (seMMP-9), hypothesis 1 (H1), hypothesis 2 (H2).

expressed (Xenodontini, Tachymenini, and Conophiini) and no common ancestral seMMP-9.

Unlike svMMP-Bs, which are hypothesized to have evolved from svMMP-As rather than seMMP-9s directly (Bayona-Serrano et al., 2020), our topology suggests svMMP-Cs may be descended from both seMMP-9s and svMMP-As (*i.e.*, Hypothesis 1 [H1] and Hypothesis [H2] in Fig. 3b)—perhaps via exon deletion or alternative splicing. However, the putative seMMP-9 we recovered and used in our phylogenetic analyses cannot be ruled out as a chimeric sequence. After mapping reads to this transcript, we identified areas with low coverage where reads rarely overlapped, suggestive of chimeric assembly. Although the relationships of svMMPs remained identical with the exclusion of the putative seMMP-9, additional sampling and sequencing is needed to estimate a more robust evolutionary history of the newly described svMMP-C.

Although the precise role of svMMPs remains undetermined, it is likely they serve as tissue degradation agents given that their homologs typically degrade extracellular matrix proteins in a variety of physiological and pathological pathways (Modahl and Mackessy, 2019 and references therein). Bayona-Serrano et al. (2020) found similar proteolytic activity in both svMMP- and SVMP-rich xenodontine venoms, suggesting some functional redundancy and replacement. Notably, this redundancy may have increased the evolvability of some of these toxins by relaxing selection and allowing neutral variation to accumulate without compromising the venom phenotype (e.g., Jackson et al., 2019). Thus, svMMP acquisition may have enabled novel activities or taxon-specificity to evolve in the venom of these snakes (Bayona-Serrano et al., 2020). Still, many species like *C. lineatus* maintain both svMMPs and SVMPs, so there may be potential for synergistic effects between the two toxin classes in producing extracellular matrix lesions (Junqueira-de-Azevedo et al., 2016). Indeed, we have much to explore regarding the function, biological activity, and exaptive co-option or duplication of svMMPs during the evolution of rear-fanged snakes.

3.4. Other atypical venom components

Along with svMMPs, several other atypical venom proteins—Lacta, SNED, and MUC—were proteomically confirmed in the DVG secretions, suggesting possible recruitment into the venom arsenal of *C. lineatus*. Lactas are an emerging venom component of unknown function found only in the subfamily Xenodontinae (Dipsadidae). Although its exact role in the venom is unknown, a protein containing a lactadherin-like FA58C (coagulation factor V and VIII C-terminal) domain was identified and proteomically confirmed in *Thamnodynastes strigatus* venom (Ching et al., 2012). Junqueira-de-Azevedo et al. (2016) also discovered a complete transcript in the transcriptome of *Oxyrhopus guibei*. *Conophis lineatus* expressed two unique Lacta transcripts both of which were proteomically confirmed (1425 and 1410 bp, 53.80 and 53.11 kDa, signal peptides detected). Our discovery of Lactas in the venom of *C. lineatus*—a basal xenodontine—suggests that lactadherin-like proteins may have been recruited to the venom repertoire of the Xenodontinae, or possibly the Dipsadidae, early in their evolution. Lactadherin has a diverse, multifunctional role, but given its ability to affect hemostasis by inhibiting coagulation enzyme complexes (Kamińska et al., 2018), we speculate it may serve as an anticoagulant in the venom of these snakes.

Transcripts most closely matching sushi, nidogen and EGF-like domains 1 (SNED1) and mucin-5B (MUC5B) were also verified proteomically in the venom of *C. lineatus*—SNED (801 bp, 29.60 kDa, signal peptide undetected) and MUC (2892 bp, 105.26 kDa, signal peptide undetected)—but their functional roles are unknown. Due to their low abundances, it is possible they could merely represent general housekeeping proteins or contamination from the oral orifice rather than true venom components. SNED1, like other extracellular matrix proteins, probably functions by binding to cell surface receptors and interacting with other extracellular matrix proteins, thus altering signaling pathways and cellular functions (Vallet et al., 2021). Thus far, it has been implicated in craniofacial development and breast cancer metastasis, but recent investigations also revealed the potential for various SNED1-integrin interactions and a hypothesized role in signaling and regulating collagen deposition and organization (Vallet et al., 2021). Other known snake venom integrin-binding molecules—such as disintegrins and C-type lectins (Marcinkiewicz, 2013)—may alter binding and platelet activity, acting as hemorrhage-promoting and anticoagulation agents (Calvete et al., 2005; Leduc and Bon, 1998; Mackessy, 2010). Given its known properties, SNED1 may have been co-opted into the venom of *C. lineatus* as a similar means to modulate cell signaling and interfere with platelet activity.

Mucin-5B is a glycosylated, epithelial-produced protein that is secreted by mucosal surfaces (Agha-Hosseini et al., 2017). It is a prominent component of saliva, and due to its gel-forming and antimicrobial properties, it plays a role in shielding oral mucosa, lubrication, hydration, mastication, and deglutition (Agha-Hosseini et al., 2017; Petrou and Crouzier, 2018). Although the presence of mucins may be result of contamination from saliva during venom extraction, mucins can have diverse bioactive effects including the sequestration of bioactive proteins and peptides, thus modulating their bioavailability and bioactivity (Petrou and Crouzier, 2018 and sources therein). For example, cobra venom mucin, isolated from *Naja kaouthia*, does not form highly viscous aqueous solutions and interacts with several venom proteins and glycoproteins noncovalently (Gowda and Davidson, 1994). Because these mucin-associated proteins are insoluble upon separation from the venom mucin, cobra venom mucin has a suggested function of maintaining the solubility of certain venom proteins (Gowda and Davidson, 1994). As a venom component in *C. lineatus*, we speculate MUC could have been recruited to protect and support the oral epithelium of the DVG system but could also aid in prey swallowing via lubrication. However, its potential as a modulator for the solubility and bioavailability of other venom components should be further explored.

3.5. Typical venom components

SVMPs, 3FTxs, CTLs, and CRiSPs are the most ubiquitous toxin classes observed in NFFS venoms (Junqueira-de-Azevedo et al., 2016; Modahl and Mackessy, 2019). However, the venom composition of most snakes usually takes on one of two types: either an elapid-like venom dominated by smaller, often neurotoxic 3FTxs, or a viper-like venom that consists primarily of larger enzymatic proteins, such as SVMPs (Mackessy, 2010; Modahl and Mackessy, 2019). In *C. lineatus*, svMMPs, CTLs, and SVMPIIIs dominate the DVG transcriptome (86.4%), with CRiSPs, Lactas, and SVSPs constituting the principal minor components (11.7%; totaling 98.1% of the total transcribed putative venom transcripts).

CTLs are non-enzymatic proteins known to induce hemagglutination by binding to oligosaccharide moieties of platelet and collagen receptors, thus acting as anticoagulants and platelet modulators (Leduc and Bon, 1998; Mackessy, 2010; Modahl and Mackessy, 2019). CTLs are pervasive and diverse in NFFS venoms, with “true” CTL, CTL-like (snaclec), and putative new venom CTL transcripts reported (Junqueira-de-Azevedo et al., 2016). Given that these proteins have diversified greatly and possess various binding motifs, they might provide different or additional functionalities in NFFS venoms (Junqueira-de-Azevedo et al., 2016; Modahl and Mackessy, 2019). With six putative toxin transcripts, CTLs in the venom of *C. lineatus* could play multiple roles.

SVMPs are enzymes that hydrolyze many structural proteins and degrade endothelial cell membrane components, or target proteins involved in coagulation. Their bioactive effects include hemorrhage, edema, coagulopathy, blistering, inflammation, and necrosis, which likely aid in prey pre-digestion (Gutiérrez et al., 2010; Mackessy, 2010; Modahl and Mackessy, 2019). In *C. lineatus*, all five SVMP transcripts are of the P-III subclass (SVMPIIIs), which is typical among NFFSs (Junqueira-de-Azevedo et al., 2016; Modahl and Mackessy, 2019). NFFS

SVMPIIIs can be very potent as well as functionally diverse, and some might also have taxon selectivity (Modahl and Mackessy, 2019).

CRiSPs are ubiquitous non-enzymatic venom components without a clear role or biological target and are often represented by a single paralog with high expression and translation (Junqueira-de-Azevedo et al., 2016). They apparently lack proteolytic, hemorrhage, and coagulant activity and the few assessed examples have inhibited various ion channels, induced inflammation, or shown necrotic or neurotoxic activity (reviewed by Modahl and Mackessy, 2019). CRiSPs probably enact an important biological role in venom given their broad phenotypic occurrence and conserved structure (Modahl and Mackessy, 2019).

SVSPs prevail over many viper venoms (Mackessy, 2010), but are generally uncommon in NFFSs, having only been reported in dipsadids (Junqueira-de-Azevedo et al., 2016; Modahl and Mackessy, 2019). We proteomically confirmed two SVSPs in the venom of *C. lineatus*. These enzymatic venom components disrupt hemostasis and are known to both promote and inhibit blood coagulation (Mackessy, 2010; Modahl and Mackessy, 2019).

Along with the typical, ubiquitous snake venom components, *C. lineatus* co-opted a number of novel molecules to its venom arsenal as well. As previously discussed, preliminary investigations suggest enzymatic svMMPs have high proteolytic activity (Bayona-Serrano et al., 2020) and likely act as tissue degradation agents similar to SVMPs by destroying the extracellular matrix and producing local hemorrhagic effects. Similarly, Lactas likely serve as anticoagulants (e.g., Kamińska et al., 2018). Therefore, by and large, the venom of *C. lineatus* is overwhelmingly proteolytic and potentially hemorrhagic, and it resembles that of a characteristic viper, with larger enzymatic proteins dominating 70% of its venom. Several toxin families, such as CTLs and CRiSPs, are not only abundant in *C. lineatus*, but also ubiquitous in NFFSs and venomous snakes as a whole. Despite their ubiquity and abundance, few investigations have focused on these widespread toxin families and more research is needed to characterize their roles as venom components..

3.6. Venom delivery system

As is particularly evident in NFFSs, possessing a toxic venom within the oral gland is not analogous to delivering it at medically relevant

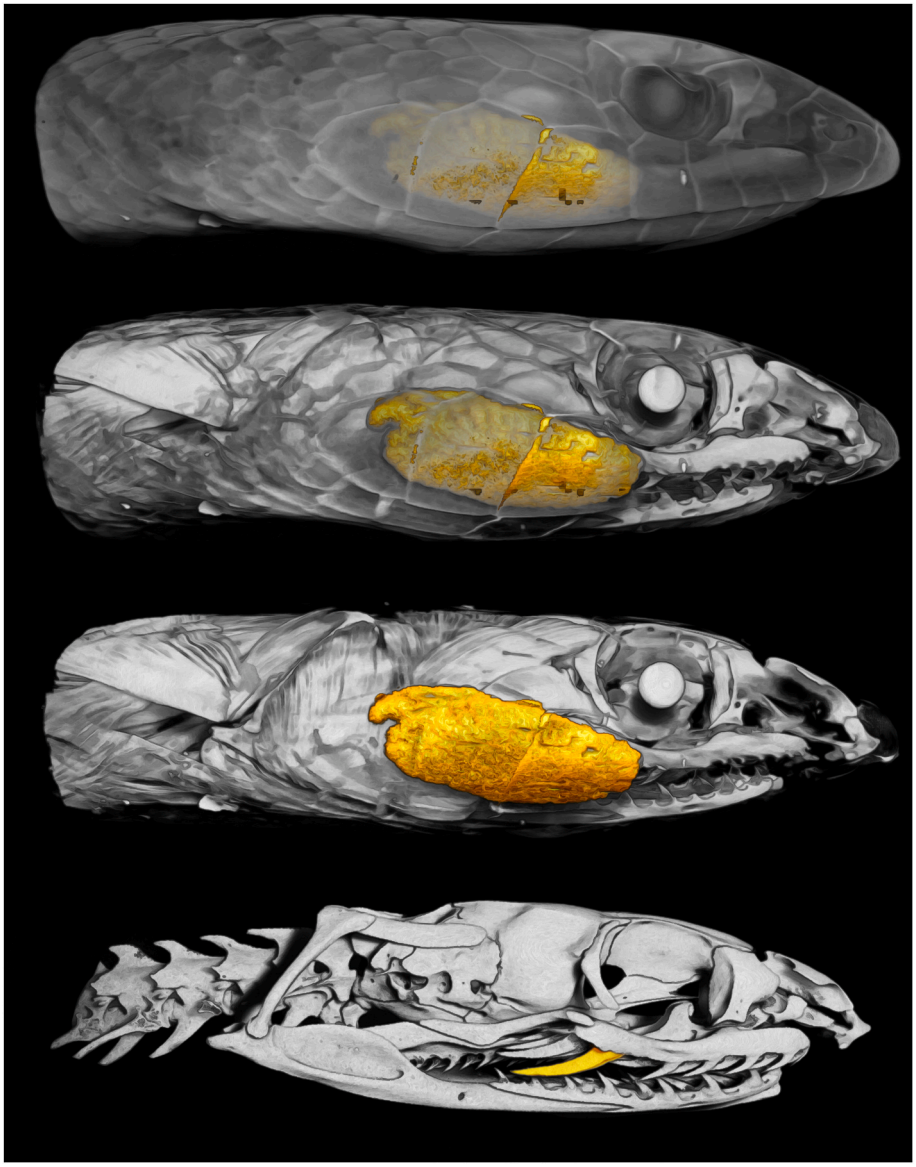

Fig. 4. Diffusible iodine-based contrast-enhanced and micro-computed tomography (diceCT and μCT) scans of *Conophis lineatus* (UMMZ 247084), with the Duvernoy's venom gland and rear-fang highlighted in yellow. (For interpretation of the references to color in this figure legend, the reader is referred to the Web version of this article.)

levels—venom apparatus, mode of delivery, composition, and potential prey specificity of the toxins therein all play a role in the venom delivery system (Weinstein et al., 2010; Westeen et al., 2020). In general, the DVG morphology corresponds to a low-pressure venom delivery system, or a reduced delivery rate and efficiency of venom secretions compared to the higher-pressure systems of front-fanged snakes (Kardong and Lavin-Murcio, 1993; Weinstein et al., 2010; but see Jackson et al., 2017). Although *C. lineatus* possesses the lower-pressure DVG system, it exhibits numerous characteristics that allow it to deliver medically relevant bites to humans. Visualizing the morphological features of the venom apparatus using diceCT and μCT, we can clearly see the considerable DVG and rear-fang size relative to head size in *C. lineatus* (Fig. 4). Although the histology of the DVG has not been studied for *C. lineatus* specifically, Taub (1967) found *C. vittatus* to possess a purely serous DVG, similar to other known medically significant NFFSs.

In regard to mode of delivery, this extremely active and fast-moving species is well-known for its adverse demeanor and tendency to bite (e.g., Ditmars, 1931; Heimes, 2016; McCranie, 2011; Neill and Allen, 1959; Savage, 2002; Wellman, 1963). Neill and Allen (1959) expressed great difficulty in handling this species without being bitten, even when held firmly behind the head. This was due to the indistinction of the snake's head from its neck and its apt ability to bring its rear-fangs toward the handler by pulling backwards or angling its head downward. Combined with this snake's sizeable rear-fangs (i.e., enlarged, grooved posterior maxillary teeth; Wellman, 1963) and large DVGs (Fig. 4), *C. lineatus* poses a formidable challenge in avoiding snakebite and envenomation during handling.

Additionally, Neill and Allen (1959) noted the very mobile maxilla of *C. lineatus*, which may effectively allow the rear-fangs to be brought forward, thus being the first teeth to engage with the recipient during a strike (e.g., Kardong, 1979). Moreover, the strikes themselves are delivered with such celerity that the motion has been described as a sudden "stabbing" or "slashing" movement (Neill and Allen, 1959; Savage, 2002). Overall, these characteristics allow *C. lineatus* to achieve envenomation more efficiently than many other NFFSs and deliver medically relevant doses to humans, bestowing this snake with notable risk potential (see below; Document S2). Undoubtedly, human envenomings and their medical significance also need to be explored in the context of venom composition and specificity—features deeply rooted in ecology.

3.7. Linking venom to potential function

Venom is intrinsically ecological, so evaluating venom through an ecological lens may provide valuable insights into its evolution and incite new hypotheses (Jackson et al., 2019). Although the primary function of venom tends to be prey subjugation—with venom complexity increasing according to dietary breadth (Holding et al., 2021)—it may also serve as a digestive aid for bulky prey items, a lubricant during ingestion, or a form of defense (Kardong, 2002; Kazandjian et al., 2021). *Conophis lineatus* is a diurnal species that forages by active pursuit, nook-probing, and excavation (Henderson and Binder, 1981; Lee, 1996; Savage, 2002; Scott, jr, 1983; Stafford and Henderson, 2006; Wellman, 1963). Overall, *C. lineatus* appears to feed indiscriminately and, thus, possesses a large, documented prey breadth including anurans, lizards, snakes, avian eggs, small mammals, and arthropods (reviewed by Pérez-Alvarado and Vásquez-Cruz, 2021; Stafford and Henderson, 2006). Although these data suggest low dietary selectivity, Stafford and Henderson (2006) found lizards—particularly teiids—and arthropods to be the most important taxonomic prey groups of *C. lineatus* (ssp. *concolor*) from the Yucatán Peninsula.

Studying the prey handling of *C. lineatus* may also provide insights as to whether its venom has any selective taxonomic targets. Despite few wild observations, *C. lineatus* has been noted for its brutal interaction with other snakes. Ditmars (1931) specifically described this species as "savage" in the way it imbedded its fangs and delivered "benumbing poison" into a young false fer-de-lance (*Xenodon rabdocephalus*). Mittleman (1944) detailed several instances of captive feeding, in which two relatively large Common Gartersnakes (*Thamnophis sirtalis*) and several Dekay's Brownsnakes (*Storeria dekayi*) were dispatched by the bites of a *C. lineatus*. Similarly, Rodriguez Garcia et al. (1998) indicated that *C. lineatus* was the only species to attack and predate the ophiophagous (and lengthier) coral snakes (*Micrurus diastema* and *M. limbatus*) during their feeding trials.

Interestingly, behavioral differences seemingly exist among feeding observations—with some prey bitten and held until quiescent (Mays, 2010; Savage, 2002), others bitten and apparently constricted (Ditmars, 1931; Gómez-de-Regil and Escalante-Pasos, 2017; Hernández-Gallegos et al., 2008), and some quickly bitten and released, left to bleed out or succumb to the venom (Mittleman, 1944). To emphasize, toxin specificity may be paired with differences in behaviors or predatory modes toward different prey (Weinstein et al., 2010). Therefore, natural history observations of this species are non-trivial and may aid in deciphering the specific roles of certain venom components.

Though often overlooked, it is important to point out that the venom and autecology of *C. lineatus* may have also evolved to complement each other. For instance, it is hypothesized that the high enzymatic toxin content of its venom would be rate-limited by temperature (Jackson et al., 2019), perhaps constraining the trophic niche by favoring taxa (*i.e.*, homeothermic endotherms) or conditions with relatively constant temperatures. However, because *C. lineatus* hunts during the day when environmental (and ectothermic prey) temperatures are raised, the effective taxonomic-scope of its venom may expand to encompass both ecto- and endotherms. Even so, greater attention should be given to geographic variation and ontogeny in diet and venom composition to aid in elucidating potential taxon specificity and function.

Despite their limitations, the best evidence available on the biological effects and perhaps function of *Conophis* venom may come from envenomation case reports. Although *Conophis* is well-known for its potent bite—as can be gathered from the numerous anecdotal reports in the literature (Campbell, 1998; Ditmars, 1931; Greding jr., 1972; Gutiérrez and Sasa, 2002; HerpetoNica, 2015; Johanbocke, 1974; Johnson, 1988; Lee, 1996; Marineros, 2000; McCranie, 2011; Mertens, 1952; Savage, 2002; Scott, jr, 1983; Taylor and Smith, 1938; Weinstein et al., 2011; Wellman, 1963)—no detailed medical case studies are published (Table 1; Document S2). Of those reports, bite symptoms varied widely from uncomplicated mechanical trauma from the teeth (no envenoming, 24%) to somewhat severe local envenomings of which the most commonly reported symptoms included: substantial local edema (65%) that may extend to the entire bitten extremity, pain (65%), and persistent bleeding (56%) at the bite site (see Document S2 for more details). However, erythema (18%), numbness (15%), ecchymosis (12%), aching (6%), cephalgia (6%), serosanguinous drainage (6%), soreness (6%), stiffness (6%), abnormal blood work (3%), digital weakness (3%), hematoma (3%), hyperalgesia (3%), localized cramping (3%), local lymphadenopathy (3%), nausea (3%), paresthesia ('tingling') at the top of the head (3%), and vomiting (3%) have also been reported (Table 1; Document S2). Given the observed sequelae, it also seems reasonable that some hospitalized bites may have been misattributed to viperids and treated as such (e.g., de Medeiros et al., 2021; Villca-Corani et al., 2021).

Overall, the witnessed biological activity of *Conophis* venom on humans adheres to many of the expected effects of its major components, but more detailed clinical cases are needed to clarify specific symptoms (Document S2). Given the persistent bleeding often associated with the bite wound, it is likely that one or more venom components act as anticoagulants as has been suggested by several authors (Campbell, 1998; Gutiérrez and Sasa, 2002; McCranie, 2011; Scott, jr, 1983). Careful observation of both human and prey envenomation outcomes and functional assays are still needed to help further disentangle the function and biological activities of the various *Conophis* venom components, but it is quite clear that great caution should be

Table 1
Subjective *Conophis* envenomation symptomatology summary, including species, geographic location (origin), bite placement, reported effects, and the data source(s). Asterisks (*) denote information based on assumption. Definitions: external hemorrhage, superficial (local) bleeding; edema, swelling; erythema, skin redness; ecchymosis, bruising; cephalgia, headache; serosanguinous drainage, oozing or discharging wound; lymphadenopathy, swollen or tender lymph nodes; paresthesia, tingling or pins and needles sensation; hyperalgesia, hypersensitivity to pain. Abbreviations: R, right; L, left; SFP, single fang puncture; PB, protracted bite (chewing); Y, yes; N, no; hr(s), hour(s); min, minute(s); wk(s), week(s); mo(s), month(s). Greater detail and interpretations per case can be found in Document S2.

			Reported Effects [Persistence or Details]:							
Conophis Species	Geographic Location	Bite Placement [Details]	Envenoming	External Hemorrhage	Pain	Edema	Erythema	Ecchymosis	Other Symptoms and Notes	Source(s)
lineatus	Honduras*	Hand*	Y		Y [several hrs]	Y [several hrs]				Douglas March in Ditmars (1931)
vittatus	Xaltianguis, Guerrero, Mexico	Ring finger [middle joint]	Y		Y [some time]	Y [some time]			digital weakness [1.5+ yrs]; some lasting digital damage decades later	Taylor and Smith (1938); E. H. Taylor in Wellman (1963)
lineatus	San Salvador, El Salvador	Hand	Y	Y [1 hr]						"gardener" in Mertens (1952)
sp.	–	Hand	Y		Y [several hrs]	Y [several hrs]				William E. Duellman in Wellman (1963)
lineatus	Veracruz, Mexico	Forefinger	Y		Y [1 hr]	Y [24 hrs]				Dale L. Hoyt in Wellman (1963)
lineatus	Esparza, Puntarenas, Costa Rica	Hand [SFP]	Y		Y [1 hr]		Y [1 hr]		cephalgia [1 hr]	Greding (1972)
lineatus	La Union, Puntarenas, Costa Rica	Index finger [R]; middle finger [L, PB, tip]	Y	Y		Y [11 days]	Y [6 days]		progressive edema involving entire extremity (arm)	Johanbocke (1974)
lineatus	Costa Rica*	–	Y	Y* [1+ hrs]	Y*	Y*			serosanguinous drainage*; hematoma*	D. Janzen* in Scott (1983); D. Janzen in Savage (2002)
lineatus	Tulum, Quintana Roo, Mexico	Thumb [L, PB, distal knuckle]	Y	Y	Y [immediate]	Y [3 days]		Y	aching; numbness; soreness [1 mo]; local edema involving entire hand	Cook (1984); Johnson (1988)
vittatus	10 km NE of Tomatlán, Jalisco, Mexico	Index finger [R, PB, proximal joint]	Y		Y [transient]	Y [24 hrs]			local edema involving entire hand	Robert G. Webb in Johnson (1988)
lineatus	Yucatán Peninsula, Mexico*	Thumb [R, base]	Y	Y [copious]		Y [several days]			local lymphadenopathy (axillary lymph nodes); progressive edema involving entire hand and lower arm	Lee (1996)
lineatus	Pacific Coast of Guatemala	Thumb	Y		Y	Y [several days]		Y	progressive edema involving entire extremity (arm)	Campbell (1998)
lineatus	Honduras*	–	N						uncomplicated bite	Marineros (2000)
lineatus	Honduras*	–	N						uncomplicated bite	Marineros (2000)
lineatus	Honduras*	–	N						uncomplicated bite	Marineros (2000)
lineatus	Guatemala	–	Y		Y*	Y*				Manuel Acevedo in Gutierrez and Sasa (2002)*
lineatus	Santa Rosa National Park, Guanacaste, Costa Rica	–	Y	Y [30 min]	Y	Y				Mahmood Sasa in Gutierrez and Sasa (2002); Mahmood

(*continued on next page*)

Table 1 (*continued*)

Conophis Species	Geographic Location	Bite Placement [Details]	Reported Effects [Persistence or Details]: Envenoming	External Hemorrhage	Pain	Edema	Erythema	Ecchymosis	Other Symptoms and Notes	Source(s)
										Sasa (pers. comm.)
lineatus	Honduras*	–	Y	Y [5 min]						McCranie (2011)
lineatus	Honduras*	–	Y						paresthesia ("tingling") at top of head	McCranie (2011)
lineatus	Honduras*	–	N						uncomplicated bite	McCranie (2011)
lineatus	Honduras*	–	N						uncomplicated bite	McCranie (2011)
lineatus	–	–	Y	Y [transient]		Y [2 hrs]	Y* [2 hrs]			Roy McDiarmid in Weinstein et al. (2011)
lineatus	–	–	Y	Y [transient]		Y [2 hrs]	Y* [2 hrs]			Roy McDiarmid in Weinstein et al. (2011)
lineatus	Playa Ocotal, Guanacaste, Costa Rica	Interdigit webbing b/w index and middle finger [R, PB]	Y	Y [1 hrs]	Y [2 wks]	Y [3 days]			mild pain progressively worsened with swelling; full function of hand regained after 1 mo; middle knuckle remained swollen for 6+ mos; local edema involving entire hand	Paul Dixon (pers. comm.)
lineatus	La Laguna El Jocotal, El Salvador	Index finger [PB*, base]	Y		Y	Y [24 hrs]			local edema involving entire hand	Lee A. Fitzgerald (pers. comm.)
vittatus	Colima, Colima, Mexico	Index finger [L, PB]	Y	Y [1+ hr*]	Y [1 day]	Y [5 days]		Y [5 days]	immediate stinging progressed to intense throbbing pain within 1 hr; hyperalgesia [12 hrs]; bruising blue in color [12–16 hrs], but turned abnormally green [1.5 days]; serosanguinous drainage [12 hrs]; abnormal blood work 1–2 mos later*	Cristoph Grünwald (pers. comm.)
lineatus	Puente Nacional, Veracruz, Mexico	Little finger [× 2]	Y	Y [a few hrs]	Y	Y [1 hr]			aching [1 hr]; numbness [2 days]; stiffness [2 days]	David M. Hillis (pers. comm.)
lineatus	55 km N of Siguatepeque, Santa Barbara, Honduras	Wrist [R, × 2, PB]; index finger [L, base]; index finger [R, SFP, tip]	Y	Y [several hrs]	Y	Y [1 day]			numbness [5 hrs] in index finger (R); soreness [5+ hrs] in wrist	David M. Hillis (pers. comm.)
vittatus	Mexico	Finger	N	Y [< 1 min]	Y				minor effects due to physical damage inflicted by teeth; uncomplicated bite	Gunther Köhler (pers. comm.)
lineatus	Honduras	Finger	N	Y [< 1 min]	Y				minor effects due to physical damage inflicted by teeth; uncomplicated bite	Gunther Köhler (pers. comm.)
lineatus	Nicaragua	Finger	N	Y [< 1 min]	Y				minor effects due to physical damage inflicted by teeth; uncomplicated bite	Gunther Köhler (pers. comm.)
lineatus	Caimital, Nicoya, Guanacaste, Costa Rica	Index finger [R]	Y	Y [4.5 hrs]	Y [1+ day]	Y [11+ hrs]	Y [11+ hrs]		cephalgia [2.5+ hrs]; localized cramping [2.5+ hrs]; nausea [2.5 hrs]; vomiting [×1]; numbness [1+ day]; stiffness [1+	Jean Francisco Montero Castrillo (pers. comm.)

(*continued on next page*)

Table 1 (*continued*)

Conophis Species	Geographic Location	Bite Placement [Details]	Reported Effects [Persistence or Details]: Envenoming	External Hemorrhage	Pain	Edema	Erythema	Ecchymosis	Other Symptoms and Notes	Source(s)
									day]; stinging followed by excruciating, radiating pain within 1 hr; progressive edema extending to elbow	
lineatus	Tejona, Guanacaste, Costa Rica	Index finger [L]	Y	Y [25 min]	Y [1 day]	Y [1 day]	Y [1 day]		numbness [1 wk]	Ray Morgan (pers. comm.)
lineatus	Rus, Gracias a Dios, Honduras	Thumb [SFP]	Y	Y [1 day]	Y [6–8 hrs]	Y [6–8 hrs]		Y [1+ wk]	burning followed by throbbing pain	Josiah H. Townsend (pers. comm.)

taken with *Conophis* spp. (see Document S2 for recommendations).

4. Conclusions

The venom of many species remains unexplored due to difficulties in obtaining adequate venom yields. This is particularly true for small taxa such as spiders, scorpions, and centipedes; but also includes NFFSs with a low-pressure venom delivery system. Yet, NFFSs make up over two-thirds of all snake diversity. Fortunately, next-generation sequencing has greatly facilitated our ability to study these species and not only highlight the diversity of toxins present, but also elucidate how venoms evolve and unlock their therapeutic and diagnostic potential (Mackessy, 2002; Modahl et al., 2020). However, to judge the medical relevance of a taxon, it is important to understand the venom delivery system in its entirety. Thus, we combined transcriptomics, proteomics, high-resolution computed tomography, natural history, and envenomation cases to examine the venom apparatus, mode of delivery, composition, and specificity of *C. lineatus*. Using these methodologies, we highlight the overwhelming presence of a recently discovered toxin family, svMMPs, in *C. lineatus* including a unique isoform. Among typical snake toxin families like SVMPIIIs and CTLs, we also identified the presence of Lactas, SNED, and MUC in the venom of *C. lineatus*. Although the function and role of these nascent venom components remains unknown and purely speculative, they warrant further consideration, as the properties of related molecules are being bio-prospected in disease, cancer, and biomaterials research (e.g., Kamińska et al., 2018; Petrou and Crouzier, 2018; Vallet et al., 2021). Indeed, many snake venom components offer potential therapeutic and diagnostic applications (reviewed by Modahl et al., 2020). Our results highlight that even a single specimen of a previously unstudied species can have large impacts on our understanding of venom evolution and toxin discovery.

Ethical statement

Reporting standards

The authors declare that our manuscript describes original research and every effort was made to ensure the accuracy of the results and the account.

Data access and retention

Raw data for the single *C. lineatus* Duvernoy's venom gland transcriptome were submitted to the National Center for Biotechnology Information (NCBI) Sequence Read Archive (SRA) accession SRR14319401(BioSample: SAMN18863723; BioProject: PRJNA88989). The final transcriptome was submitted to the NCBI Transcriptome Shotgun Assembly (TSA) database, and the project deposited at DDBJ/EMBL/GenBank under the accession GJFD00000000. The version described in this paper is the first version, GJFD01000000.

Originality and plagiarism

The authors declare that our manuscript is an original work with proper citations as needed.

Multiple, redundant or concurrent publication

The authors declare that the data and work described in our manuscript has not and will not be submitted for consideration to another journal.

Acknowledgment of sources

The authors have provided proper acknowledgment of sources to the best of their abilities.

Author contributions

Conceptualization, **TDS**, **RMR** and **CLP**; Methodology, **TDS** and **RMR**; Software, **DRR**; Validation, **JDBS**; Formal Analysis, **TDS**, **RMR**, and **JDBS**; Investigation, **TDS**, **RMR**, **JDBS**, **GSN**, **TRW**; Resources, **GSN**, **TRW**, **JAOM**, **BSA**, **MMM**, **MB**, **ILMJA**, **DRR**; Data Curation, **TDS** and **RMR**; Writing – Original Draft Preparation, **TDS**, **RMR** and **CLP**; Writing – Review & Editing, **JDBS**, **GSN**, **TRW**, **JAOM**, **BSA**, **MMM**, **MB**, **ILMJA**, **DRR**, and **CLP**; Visualization, **TDS** and **TRW**; Supervision, **CLP**; Project Administration, **CLP**; Funding Acquisition, **ILMJA**, **DRR**, and **CLP**.

Authorship of paper

All authors of the manuscript made significant contributions, and no one making significant contributions was excluded from authorship. All authors have seen and read the submitted version of the manuscript and have approved submission.

Hazards and human or animal subjects

The authors hereby state that all procedures involving animals were conducted in a humane and ethical manner. Scientific collecting permits were issued by the Secretaria de Medio Ambiente y Recursos Naturales of the Estados Unidos Mexicanos (SEMARNAT; SGPA-DGVS-002288-18). All interactions with animals were approved by Clemson University's Institutional Animal Care and Use Committee under protocol 2017–067 and followed standard AVMA guidelines (Leary et al., 2013) as well as the American Society of Ichthyologists and Herpetologists

ethical guidelines. All interactions with humans were approved by Clemson University's Institutional Review Board under protocol IRB 2021-0464.

Disclosure and conflicts of interest

The authors declare that they have no known competing financial interests or personal relationships that could have appeared to influence the work reported in this paper. The authors declare no conflict of interest.

Fundamental errors in published works

If a fundamental error or inaccuracy is discovered in the results, the authors will immediately notify the editor or publisher.

Funding

This work was funded by the National Science Foundation (DEB 1822417 to CLP and DEB 1638902 to DRR), the Fundação de Amparo à Pesquisa do Estado de São Paulo (FAPESP; 2016/50127–5 and 2018/26520–4 to ILMJA), the Consejo Nacional de Ciencia y Tecnologia (CONACYT 247437 to MB) and Clemson University through faculty start-up to CLP. Creation of datasets accessed on MorphoSource was made possible by the following funders and grant numbers: NSF DBI-1701713; oVert TCN; and NSF DBI-1701714.

Declaration of competing interest

The authors declare the following financial interests/personal relationships which may be considered as potential competing interests: Christopher Parkinson reports financial support was provided by National Science Foundation. Darin Rokyta reports financial support was provided by National Science Foundation. Inacio L. M. Junqueira de Azevedo reports financial support was provided by Fundação de Amparo à Pesquisa do Estado de São Paulo. Miguel Bora reports financial support was provided by Consejo Nacional de Ciencia y Tecnologia.

Acknowledgments

We thank Edward A. Myers for his suggestions which greatly improved this manuscript, and Andrew M. Durso for literature translation assistance. We also thank Clemson University for generously providing computational resources on the Palmetto HPC Cluster. We extend our gratitude to Paul Dixon, Lee Fitzgerald, Christoph Grünwald, David Hillis, Gunther Köhler, Jean Francisco Montero Castrillo, Ray Morgan, Mahmood Sasa, and Josiah Townsend for providing information about their *Conophis* bites, and Tom Sinclair for providing obscure literature. The University of Michigan Museum of Zoology provided access to these CT data, the collection of which was funded by NSF DBI-1701713, oVert TCN, and NSF DBI-1701714. The files were downloaded from www.MorphoSource.org, Duke University. Finally, we thank the anonymous reviewers that provided helpful comments and suggestions that improved the quality of this work.

Appendix A. Supplementary data

Supplementary data to this article can be found online at https://doi.org/10.1016/j.toxicon.2021.11.009.

References

Agha-Hosseini, F., Imanpour, M., Mirzaii-Dizgah, I., Moosavi, M.S., 2017. Mucin 5B in saliva and serum of patients with oral lichen planus. Sci. Rep. 7, 5–10. https://doi.org/10.1038/s41598-017-12157-1.

Bayona-Serrano, J.D., Grazziotin, F.G., Barros-de-Carvalho, G.A., Campos, P.F., Junqueira-de-Azevedo, I.L.M., 2019. SVMMPs as an important component of the venom gland transcriptome in the genus *Erythrolamprus*. Toxicon 168, S15. https://doi.org/10.1016/j.toxicon.2019.06.077.

Bayona-Serrano, J.D., Viala, V.L., Rautsaw, R.M., Schramer, T.D., Barros-Carvalho, G.A., Nishiyama, M.Y., Freitas-de-Sousa, L.A., Moura-da-Silva, A.M., Parkinson, C.L., Grazziotin, F.G., Junqueira-de-Azevedo, I.L.M., 2020. Replacement and parallel simplification of nonhomologous proteinases maintain venom phenotypes in rear-fanged snakes. Mol. Biol. Evol. 37, 3563–3575. https://doi.org/10.1093/molbev/msaa192.

Borja, M., Neri-Castro, E., Pérez-Morales, R., Strickland, J., Ponce-López, R., Parkinson, C.L., Espinosa-Fematt, J., Sáenz-Mata, J., Flores-Martínez, E., Alagón, A., Castañeda-Gaytán, G., 2018. Ontogenetic change in the venom of Mexican black-tailed rattlesnakes (*Crotalus molossus nigrescens*). Toxins (Basel). 10, 501. https://doi.org/10.3390/toxins10120501.

Callahan, S., Crowe-Riddell, J.M., Nagesan, R.S., Gray, J.A., Davis Rabosky, A.R., 2021. A guide for optimal iodine staining and high-throughput diceCT scanning in snakes. Ecol. Evol. 1–17. https://doi.org/10.1002/ece3.7467.

Calvete, J.J., Marcinkiewicz, C., Monleón, D., Esteve, V., Celda, B., Juárez, P., Sanz, L., 2005. Snake venom disintegrins: evolution of structure and function. Toxicon 45, 1063–1074. https://doi.org/10.1016/j.toxicon.2005.02.024.

Campbell, J.A., 1998. Amphibians and Reptiles of Northern Guatemala, the Yucatán, and Belize, Animal Natural History. University of Oklahoma Press, Norman, Oklahoma.

Ching, A.T.C., Paes Leme, A.F., Zelanis, A., Rocha, M.M.T., Furtado, M.D.F.D., Silva, D. A., Trugilho, M.R.O., Da Rocha, S.L.G., Perales, J., Ho, P.L., Serrano, S.M.T., Junqueira-De-Azevedo, I.L.M., 2012. Venomics profiling of *Thamnodynastes strigatus* unveils matrix metalloproteinases and other novel proteins recruited to the toxin arsenal of rear-fanged snakes. J. Proteome Res. 11, 1152–1162. https://doi.org/10.1021/pr200876c.

Conroy, C.J., Papenfuss, T., Parker, J., Hahn, N.E., 2009. Use of tricaine methanesulfonate (MS222) for euthanasia of reptiles. J. Am. Assoc. Lab. Anim. Sci. 48, 28–32.

Cook, D.G., 1984. A case of envenomation by the neotropical colubrid snake, *Stenorrhina freminvillei*. Toxicon 22, 823–827. https://doi.org/10.1016/0041-0101(84)90168-5.

da Graça Salomão, M., Pinto Albolea, A.B., Almeida Santos, S.M., 2003. Colubrid snakebite: a public health problem in Brazil. Herpetol. Rev. 34, 307–312.

Dashevsky, D., Debono, J., Rokyta, D., Nouwens, A., Josh, P., Fry, B.G., 2018. Three-finger toxin diversification in the venoms of cat-eye snakes (Colubridae: *Boiga*). J. Mol. Evol. 86, 531–545. https://doi.org/10.1007/s00239-018-9864-6.

de Medeiros, C.R., Duarte, M.R., de Souza, S.N., 2021. Differential diagnosis between venomous (*Bothrops jararaca*, serpentes, viperidae) and "nonvenomous" (*Philodryas olfersii*, serpentes, Dipsadidae) snakebites: is it always possible? Wilderness Environ. Med. https://doi.org/10.1016/j.wem.2021.07.009.

Ditmars, R.L., 1931. Snakes of the World. The Macmillan Company, New York, New York.

Fry, B.G., Vidal, N., Norman, J.A., Vonk, F.J., Scheib, H., Ramjan, S.F.R., Kuruppu, S., Fung, K., Hedges, S.B., Richardson, M.K., Hodgson, W.C., Ignjatovic, V., Summerhayes, R., Kochva, E., 2006. Early evolution of the venom system in lizards and snakes. Nature 439, 584–588. https://doi.org/10.1038/nature04328.

Fu, L., Niu, B., Zhu, Z., Wu, S., Li, W., 2012. CD-HIT: accelerated for clustering the next-generation sequencing data. Bioinformatics 28, 3150–3152. https://doi.org/10.1093/bioinformatics/bts565.

Gómez-de-Regil, G.M., Escalante-Pasos, J.A., 2017. Nature notes: *Conophis lineatus* (duméril, bibron & duméril, 1854) diet. Mesoamerican Herpetol 4, 180–181.

Gowda, D.C., Davidson, E.A., 1994. Isolation and characterization of novel mucin-like glycoproteins from cobra venom. J. Biol. Chem. 269, 20031–20039. https://doi.org/10.1016/s0021-9258(17)32123-3.

Grabherr, M.G., Haas, B.J., Yassour, M., Levin, J.Z., Thompson, D.A., Amit, I., Adiconis, X., Fan, L., Raychowdhury, R., Zeng, Q., Chen, Z., Mauceli, E., Hacohen, N., Gnirke, A., Rhind, N., Di Palma, F., Birren, B.W., Nusbaum, C., Lindblad-Toh, K., Friedman, N., Regev, A., 2011. Full-length transcriptome assembly from RNA-Seq data without a reference genome. Nat. Biotechnol. 29, 644–652. https://doi.org/10.1038/nbt.1883.

Grazziotin, F.G., Zaher, H., Murphy, R.W., Scrocchi, G., Benavides, M.A., Zhang, Y.P., Bonatto, S.L., 2012. Molecular phylogeny of the new World Dipsadidae (serpentes: colubroidea): a reappraisal. Cladistics 28, 437–459. https://doi.org/10.1111/j.1096-0031.2012.00393.x.

Greding, E.J., 1972. Mordedura y alimentación de la culebra centroamericana *Conophis lineatus dunni* Smith. Rev. Biol. Trop. 20, 29–30.

Gutiérrez, J.M., Rucavado, A., Escalante, T., 2010. Snake venom metalloproteinases: biological roles and participation in the pathophysiology of envenomation. In: Mackessy, S.P. (Ed.), Handbook of Venoms and Toxins of Reptiles. CRC Press, Boca Raton, Florida, pp. 115–138.

Gutiérrez, J.M., Sasa, M., 2002. Bites and envenomations by colubrid snakes in Mexico and Central America. J. Toxicol. Toxin Rev. 21, 105–115. https://doi.org/10.1081/TXR-120004743.

Haas, B.J., Papanicolaou, A., Yassour, M., Grabherr, M., Blood, P.D., Bowden, J., Couger, M.B., Eccles, D., Li, B., Lieber, M., Macmanes, M.D., Ott, M., Orvis, J., Pochet, N., Strozzi, F., Weeks, N., Westerman, R., William, T., Dewey, C.N., Henschel, R., Leduc, R.D., Friedman, N., Regev, A., 2013. De novo transcript sequence reconstruction from RNA-seq using the Trinity platform for reference generation and analysis. Nat. Protoc. 8, 1494–1512. https://doi.org/10.1038/nprot.2013.084.

Heimes, P., 2016. Snakes of Mexico, Herpetofauna Mexicana. Edition Chimaira, Frankfurt, Germany.

Henderson, R.W., Binder, M.H., 1981. Excavating behavior in *Conophis lineatus* (serpentes: Colubridae). Herpetol. Rev. 12, 103–104.

Hernández-Gallegos, O., Rodríguez-Romero, F., Granados-González, G., Méndez, F.R., 2008. Natural history notes: *Conophis lineatus* (Road guarder). Diet. Herpetol. Rev. 39, 467.
HerpetoNica, 2015. Guía Ilustrada de Anfibios y Reptiles de Nicaragua. Ministerio del Ambiente y los Recursos Naturales (MARENA), Managua, Nicaragua.
Heyborne, W.H., Mackessy, S.P., 2021. Venoms of new World vinesnakes (*Oxybelis aeneus* and *O. fulgidus*). Toxicon 190, 22–30. https://doi.org/10.1016/j.toxicon.2020.12.002.
Hill, R.E., Mackessy, S.P., 1997. Venom yields from several species of colubrid snakes and differential effects of ketamine. Toxicon 35, 671–678. https://doi.org/10.1016/S0041-0101(96)00174-2.
Hofmann, E.P., Rautsaw, R.M., Mason, A.J., Strickland, J.L., Parkinson, C.L., 2021. Duvernoy's gland transcriptomics of the plains black-headed snake, *Tantilla nigriceps* (squamata, Colubridae): unearthing the venom of small rear-fanged snakes. Toxins (Basel). 13, 336. https://doi.org/10.3390/toxins13050336.
Hofmann, E.P., Rautsaw, R.M., Strickland, J.L., Holding, M.L., Hogan, M.P., Mason, A.J., Rokyta, D.R., Parkinson, C.L., 2018. Comparative venom-gland transcriptomics and venom proteomics of four Sidewinder Rattlesnake (*Crotalus cerastes*) lineages reveal little differential expression despite individual variation. Sci. Rep. 8, 15534. https://doi.org/10.1038/s41598-018-33943-5.
Holding, M.L., Margres, M.J., Mason, A.J., Parkinson, C.L., Rokyta, D.R., 2018. Evaluating the performance of de novo assembly methods for venom-gland transcriptomics. Toxins (Basel). 10, 249. https://doi.org/10.3390/toxins10060249.
Holding, M.L., Strickland, J.L., Rautsaw, R.M., Hofmann, E.P., Mason, A.J., Hogan, M.P., Nystrom, G.S., Ellsworth, S.A., Colston, T.J., Borja, M., Castañeda-Gaytán, G., Grünwald, C.I., Jones, J.M., Freitas-de-Sousa, L.A., Viala, V.L., Margres, M.J., Hingst-Zaher, E., Junqueira-de-Azevedo, I.L.M., Moura-da-Silva, A.M., Grazziotin, F.G., Gibbs, H.L., Rokyta, D.R., Parkinson, C.L., 2021. Phylogenetically diverse diets favor more complex venoms in North American pitvipers. Proc. Natl. Acad. Sci. Unit. States Am. 118, e2015579118 https://doi.org/10.1073/pnas.2015579118/-/DCSupplemental.y.
Jackson, T.N.W., Jouanne, H., Vidal, N., 2019. Snake venom in context: neglected clades and concepts. Front. Ecol. Evol. 7, 1–9. https://doi.org/10.3389/fevo.2019.00332.
Jackson, T.N.W., Young, B., Underwood, G., McCarthy, C.J., Kochva, E., Vidal, N., van der Weerd, L., Nabuurs, R., Dobson, J., Whitehead, D., Vonk, F.J., Hendrikx, I., Hay, C., Fry, B.G., 2017. Endless forms most beautiful: the evolution of ophidian oral glands, including the venom system, and the use of appropriate terminology for homologous structures. Zoomorphology 136, 107–130. https://doi.org/10.1007/s00435-016-0332-9.
Johanbocke, M.M., 1974. Effects of a bite from *Conophis lineatus*. Bull. Philidelphia Herpetol. Soc. 22, 39.
Johnson, J.D., 1988. Comments on the report of envenomation by the colubrid snake *Stenorrhina freminvillei*. Toxicon 26, 519–521.
Junqueira-de-Azevedo, I.L.M., Campos, P.F., Ching, A.T.C., Mackessy, S.P., 2016. Colubrid venom composition: an -omics perspective. Toxins (Basel) 8, 230. https://doi.org/10.3390/toxins8080230.
Kalyaanamoorthy, S., Minh, B.Q., Wong, T.K.F., Von Haeseler, A., Jermiin, L.S., 2017. ModelFinder: fast model selection for accurate phylogenetic estimates. Nat. Methods 14, 587–589. https://doi.org/10.1038/nmeth.4285.
Kamińska, A., Enguita, F.J., Stępień, E., 2018. Lactadherin: an unappreciated haemostasis regulator and potential therapeutic agent. Vasc. Pharmacol. 101, 21–28. https://doi.org/10.1016/j.vph.2017.11.006.
Kardong, K.V., 2002. Colubrid snakes and Duvernoy's "venom" glands. J. Toxicol. Toxin Rev. 21, 1–19. https://doi.org/10.1081/TXR-120004739.
Kardong, K.V., 1979. "Protovipers" and the evolution of snake fangs. Evolution (N. Y). 33, 433–443.
Kardong, K.V., Lavin-Murcio, P.A., 1993. Venom delivery of snakes as high-pressure and low-pressure systems. Copeia 644–650.
Kassambara, L., 2019. Ggpubr: "Ggplot 2". Based Publication Ready Plots.
Katoh, K., Misawa, K., Kuma, K.I., Miyata, T., 2002. MAFFT: a novel method for rapid multiple sequence alignment based on fast Fourier transform. Nucleic Acids Res. 30, 3059–3066. https://doi.org/10.1093/nar/gkf436.
Katoh, K., Standley, D.M., 2013. MAFFT multiple sequence alignment software version 7: improvements in performance and usability. Mol. Biol. Evol. 30, 772–780. https://doi.org/10.1093/molbev/mst010.
Kazandjian, T.D., Petras, D., Robinson, S.D., van Thiel, J., Greene, H.W., Arbuckle, K., Barlow, A., Carter, D.A., Wouters, R.M., Whiteley, G., Wagstaff, S.C., Arias, A.S., Albulescu, L.O., von Plettenberg Laing, A., Hall, C., Heap, A., Penrhyn-Lowe, S., McCabe, C.V., Ainsworth, S., da Silva, R.R., Dorrestein, P.C., Richardson, M.K., Gutiérrez, J.M., Calvete, J.J., Harrison, R.A., Vetter, I., Undheim, E.A.B., Wüster, W., Casewell, N.R., 2021. Convergent evolution of pain-inducing defensive venom components in spitting cobras. Science 80 (371), 386–390. https://doi.org/10.1101/2020.07.08.192443.
Komori, K., Konishi, M., Maruta, Y., Toriba, M., Sakai, A., Matsuda, A., Hori, T., Nakatani, M., Minamino, N., Akizawa, T., 2006. Characterization of a novel metalloproteinase in Duvernoy's gland of *Rhabdophis tigrinus tigrinus*. J. Toxicol. Sci. 31, 157–168. https://doi.org/10.2131/jts.31.157.
Langmead, B., Salzberg, S.L., 2012. Fast gapped-read alignment with Bowtie 2. Nat. Methods 9, 357–359. https://doi.org/10.1038/nmeth.1923.
Leary, S., Underwood, W., Anthony, R., Cartner, S., Corey, D., Grandin, T., Greenacre, C., Gwaltney-Brant, S., McCrackin, M.A., Meyer, R., Miller, D., Shearer, J., Yanong, R., 2013. AVMA Guidelines for the Euthanasia of Animals: 2013 Edition. American Veterinary Medical Association, Schaumburg, IL, pp. 1–102.
Leduc, M., Bon, C., 1998. Cloning of subunits of convulxin, a collagen-like platelet-aggregating protein from *Crotalus durissus terrificus* venom. Biochem. J. 333, 389–393. https://doi.org/10.1042/bj3330389.
Lee, J.C., 1996. The Amphibians and Reptiles of the Yucatán Peninsula. Cornell University Press, Ithaca, New York.
Li, B., Dewey, C.N., 2011. RSEM: accurate transcript quantification from RNA-Seq data with or without a reference genome. BMC Bioinf. 12, 323. https://doi.org/10.1186/1471-2105-12-323.
Li, H., 2013. Aligning Sequence Reads, Clone Sequences and Assembly Contigs with BWA-MEM arXiv Prepr. arXiv1303.3997.
Mackessy, S.P., 2010. The field of reptile toxinology: snakes, lizards, and their venoms. In: Mackessy, S.P. (Ed.), Handbook of Venoms and Toxins of Reptiles. CRC Press, Boca Raton, Florida, pp. 3–23.
Mackessy, S.P., 2002. Biochemistry and pharmacology of colubrid snake venoms. J. Toxicol. - Toxin Rev. 21, 43–83. https://doi.org/10.1081/TXR-120004741.
Mackessy, S.P., Sixberry, N.M., Heyborne, W.H., Fritts, T., 2006. Venom of the Brown Treesnake, *Boiga irregularis*: ontogenetic shifts and taxa-specific toxicity. Toxicon 47, 537–548. https://doi.org/10.1016/j.toxicon.2006.01.007.
Marcinkiewicz, C., 2013. Applications of snake venom components to modulate integrin activities in cell-matrix interactions. Int. J. Biochem. Cell Biol. 45, 1974–1986. https://doi.org/10.1016/j.biocel.2013.06.009.
Margres, M.J., Rautsaw, R.M., Strickland, J.L., Mason, A.J., Schramer, T.D., Hofmann, E. P., Stiers, E., Ellsworth, S.A., Nystrom, G.S., Hogan, M.P., Bartlett, D.A., Colston, T. J., Gilbert, D.M., Rokyta, D.R., Parkinson, C.L., 2021. The Tiger Rattlesnake genome reveals a complex genotype underlying a simple venom phenotype. Proc. Natl. Acad. Sci. Unit. States Am. 118, e2014634118 https://doi.org/10.1073/PNAS.2014634118.
Marineros, L., 2000. Guía de las Serpientes de Honduras. Dirección General de Biodiversidad, Secretaría de Recursos Naturales y Ambiente, Tegucigalpa.
Mays, J.D., 2010. Natural history notes: *Conophis lineatus* (Road guarder). Diet. Herpetol. Rev. 41, 500.
McCranie, J.R., 2011. The snakes of Honduras: systematics, distribution, and conservation. Contributions to Herpetology. Society for the Study of Amphibians and Reptiles.
McGivern, J.J., Wray, K.P., Margres, M.J., Couch, M.E., Mackessy, S.P., Rokyta, D.R., 2014. RNA-seq and high-definition mass spectrometry reveal the complex and divergent venoms of two rear-fanged colubrid snakes. BMC Genom. 15, 1061. https://doi.org/10.1186/1471-2164-15-1061.
Mertens, R., 1952. Die Amphibien und Reptilien von El Salvador, auf Grund der Reisen von R. Mertens und A. Zilch. Abh. Senckenb. Natforsch. Ges. 487, 1–120.
Minh, B.Q., Schmidt, H.A., Chernomor, O., Schrempf, D., Woodhams, M.D., Von Haeseler, A., Lanfear, R., Teeling, E., 2020. IQ-TREE 2: new models and efficient methods for phylogenetic inference in the genomic era. Mol. Biol. Evol. 37, 1530–1534. https://doi.org/10.1093/molbev/msaa015.
Minton, S.A., 1990. Venomous bites by nonvenomous snakes: an annotated bibliography of colubrid envenomation. J. Wilderness Med. 1, 119–127. https://doi.org/10.1580/0953-9859-1.2.119.
Mittleman, M.B., 1944. Feeding habits of a central American opisthoglyph snake. Copeia 122. https://doi.org/10.2307/1438771.
Modahl, C.M., Brahma, R.K., Koh, C.Y., Shioi, N., Kini, R.M., 2020. Omics technologies for profiling toxin diversity and evolution in snake venom: impacts on the discovery of therapeutic and diagnostic agents. Annu. Rev. Anim. Biosci. 8, 91–116. https://doi.org/10.1146/annurev-animal-021419-083626.
Modahl, C.M., Frietze, S., Mackessy, S.P., 2018a. Transcriptome-facilitated proteomic characterization of rear-fanged snake venoms reveal abundant metalloproteinases with enhanced activity. J. Proteomics 187, 223–234. https://doi.org/10.1016/j.jprot.2018.08.004.
Modahl, C.M., Mackessy, S.P., 2019. Venoms of rear-fanged snakes: new proteins and novel activities. Front. Ecol. Evol. 7, 1–18. https://doi.org/10.3389/fevo.2019.00279.
Modahl, C.M., Mrinalini, Frietze, S., Mackessy, S.P., 2018b. Adaptive evolution of distinct prey-specific toxin genes in rear-fanged snake venom. Proc. R. Soc. B Biol. Sci. 285, 20181003. https://doi.org/10.1098/rspb.2018.1003.
Neill, W.T., Allen, E.R., 1959. Studies on the Amphibians and reptiles of British Honduras. Publ. Res. Div. Ross Allen's Reptil. Inst. 2, 1–76.
Nguyen, L.T., Schmidt, H.A., Von Haeseler, A., Minh, B.Q., 2015. IQ-TREE: a fast and effective stochastic algorithm for estimating maximum-likelihood phylogenies. Mol. Biol. Evol. 32, 268–274. https://doi.org/10.1093/molbev/msu300.
Pedersen, T.L., 2020. Patchwork: the Composer of Plots.
Pérez-Alvarado, C.J., Vásquez-Cruz, V., 2021. Updates on the diet items of *Conophis lineatus* (squamata: Dipsadidae). Caldasia 43, 197–201. https://doi.org/10.15446/caldasia.v43n1.83517.
Petersen, T.N., Brunak, S., Von Heijne, G., Nielsen, H., 2011. SignalP 4.0: discriminating signal peptides from transmembrane regions. Nat. Methods 8, 785–786. https://doi.org/10.1038/nmeth.1701.
Petrou, G., Crouzier, T., 2018. Mucins as multifunctional building blocks of biomaterials. Biomater. Sci. 6, 2282–2297. https://doi.org/10.1039/c8bm00471d.
Prado-Franceschi, J., Hyslop, S., 2002. South American colubrid evenomations. J. Toxicol. Toxin Rev. 21, 117–158.
R Core Team, 2013. R: A Language and Environment for Statistical Computing.
Rice, P., Longden, I., Bleasby, A., 2000. EMBOSS: the European molecular biology open software suite. Trends Genet. 16, 276–277. https://doi.org/10.1016/s0168-9525(00)02024-2.
Rodriguez Garcia, J., Perez-Higareda, G., Smith, H.M., Chiszar, D., 1998. Natural history notes: *Micrurus diastema* and *M. limbatus* (diastema coral snake and tuxtlan coral snake, respectively). Diet. Herpetol. Rev. 29, 45.
Rokyta, D.R., Lemmon, A.R., Margres, M.J., Aronow, K., 2012. The venom-gland transcriptome of the eastern diamondback rattlesnake (*Crotalus adamanteus*). BMC Genom. 13, 1–23. https://doi.org/10.1186/1471-2164-13-312.

Rokyta, D.R., Margres, M.J., Ward, M.J., Sanchez, E.E., 2017. The genetics of venom ontogeny in the Eastern Diamondback Rattlesnake (*Crotalus adamanteus*). PeerJ 5, e3249. https://doi.org/10.7717/peerj.3249.

Rokyta, D.R., Wray, K.P., Margres, M.J., 2013. The genesis of an exceptionally lethal venom in the timber rattlesnake (*Crotalus horridus*) revealed through comparative venom-gland transcriptomics. BMC Genom. 14, 394. https://doi.org/10.1186/1471-2164-14-394.

Rokyta, D.R., Wray, K.P., McGivern, J.J., Margres, M.J., 2015. The transcriptomic and proteomic basis for the evolution of a novel venom phenotype within the Timber Rattlesnake (*Crotalus horridus*). Toxicon 98, 34–48. https://doi.org/10.1016/j.toxicon.2015.02.015.

Rosenberg, H.I., 1992. An improved method for collecting secretion from Duvernoy's gland of colubrid snakes. Copeia 244–246.

Rotenberg, D., Bamberger, E.S., Kochva, E., 1971. Studies on ribonucleic acid synthesis in the venom glands of *Vipera palaestinae* (Ophidia, Reptilia). Biochem. J. 121, 609–612.

Savage, J.M., 2002. The Amphibians and Reptiles of Costa Rica: A Herpetofauna between Two Continents, between Two Seas. University of Chicago Press, Chicago, Illinois.

Scott, N.J., 1983. *Conophis lineatus* Guarda camino. In: Janzen, D.H. (Ed.), Costa Rican Natural History. The University of Chicago Press, Chicago, pp. 392–393.

Stafford, P.J., Henderson, R.W., 2006. Ecological traits of the colubrid snake Conophis lineatus concolor (Guarda Camino) in the Yucatán peninsula. South Am. J. Herpetol. 1, 210–217. https://doi.org/10.2994/1808-9798(2006)1[210:etotcs]2.0.co;2.

Taub, A.M., 1967. Comparative histological studies on Duvernoy's gland of colubrid snakes. Bull. Am. Mus. Nat. Hist. 138, 1–50.

Taylor, E.H., Smith, H.M., 1938. Miscellaneous notes on Mexican snakes. Univ. Kans. Sci. Bull. 25, 239–258.

Uetz, P., 2010. The original descriptions of reptiles. Zootaxa 2334, 59–68.

Uetz, P., Freed, P., Hošek, J., 2020. The Reptile Database [WWW Document]. http://www.reptile-database.org. accessed 2.24.21.

Uetz, P., Stylianou, A., 2018. The original descriptions of reptiles and their subspecies. Zootaxa 4375, 257–264. https://doi.org/10.11646/zootaxa.4375.2.5.

Vallet, S.D., Davis, M.N., Barqué, A., Ricard-Blum, S., Naba, A., 2021. Computational and experimental characterization of the novel ECM glycoprotein SNED1 and prediction of its interactome. Biochem. J. 478, 1413–1434. https://doi.org/10.1101/2020.07.27.223107.

Vidal, N., 2002. Colubroid systematics: evidence for an early appearance of the venom apparatus followed by extensive evolutionary tinkering. J. Toxicol. Toxin Rev. 21, 21–41. https://doi.org/10.1081/TXR-120004740.

Villca-Corani, H., Nieto-Ariza, B., León, R., Rocabado, J.A., Chippaux, J.P., Urra, F.A., 2021. First reports of envenoming by South American water snakes *Helicops angulatus* and *Hydrops triangularis* from Bolivian Amazon: a one-year prospective study of non-front-fanged colubroid snakebites. Toxicon 202, 53–59. https://doi.org/10.1016/j.toxicon.2021.09.003.

Vonk, F.J., Admiraal, J.F., Jackson, K., Reshef, R., De Bakker, M.A.G., Vanderschoot, K., Van Den Berge, I., Van Atten, M., Burgerhout, E., Beck, A., Mirtschin, P.J., Kochva, E., Witte, F., Fry, B.G., Woods, A.E., Richardson, M.K., 2008. Evolutionary origin and development of snake fangs. Nature 454, 630–633. https://doi.org/10.1038/nature07178.

Warrell, D.A., 2004. Snakebites in central and south America: epidemiology, clinical features, and clinical management. In: Campbell, J.A., Lamar, W.W. (Eds.), The Venomous Reptiles of the Western Hemisphere. Cornell University Press, Ithaca, New York, pp. 709–761.

Weinstein, S.A., Smith, T.L., Kardong, K.V., 2010. Reptile venom glands: form, function, and future. In: Mackessy, S.P. (Ed.), Handbook of Venoms and Toxins of Reptiles. CRC Press, Boca Raton, Florida, pp. 65–91.

Weinstein, S.A., Warrell, D.A., White, J., Keyler, D.E., 2011. "Venomous" Bites from Non-venomous Snakes: A Critical Analysis of Risk and Management of "Colubrid" Snake Bites, first ed. Elsevier Inc., London, UK https://doi.org/10.1016/C2010-0-68461-6.

Wellman, J., 1963. A revision of snakes of the genus *Conophis* (family Colubridae, from Middle America). Univ. Kans. Publ. Mus. Nat. Hist. 15, 251–295.

Westeen, E.P., Durso, A.M., Grundler, M.C., Rabosky, D.L., Davis Rabosky, A.R., 2020. What makes a fang? Phylogenetic and ecological controls on tooth evolution in rear-fanged snakes. BMC Evol. Biol. 20, 1–15. https://doi.org/10.1186/s12862-020-01645-0.

Wickham, H., François, R., Henry, L., Müller, K., 2020. Dplyr: A Grammar of Data Manipulation.

Wilson, L.D., Johnson, J.D., 2012. Distributional patterns of the herpetofauna of mesoamerica, a biodiversity hotspot. In: Wilson, L.D., Townsend, J.H., Johnson, J.D. (Eds.), Conservation of Mesoamerican Amphibians and Reptiles. Eagle Mountain Publishing, LC, Eagle Mountain, Utah, pp. 30–235.

Zaher, H., Murphy, R.W., Arredondo, J.C., Graboski, R., Machado-Filho, P.R., Mahlow, K., Montingelli, G.G., Quadros, A.B., Orlov, N.L., Wilkinson, M., Zhang, Y. P., Grazziotin, F.G., 2019. Large-scale molecular phylogeny, morphology, divergence-time estimation, and the fossil record of advanced caenophidian snakes (Squamata: serpentes). PLoS One 14, e0216148. https://doi.org/10.1371/journal.pone.0216148.

Zhang, J., Kobert, K., Flouri, T., Stamatakis, A., 2014. PEAR: a fast and accurate Illumina Paired-End reAd mergeR. Bioinformatics 30, 614–620. https://doi.org/10.1093/bioinformatics/btt593.